USING INVERSE EULER EQUATIONS TO SOLVE MULTIDIMENSIONAL DISCRETE-CONTINUOUS DYNAMIC MODELS: A GENERAL METHOD[‡]

LORETTI I. DOBRESCU[*] AND AKSHAY SHANKER[†]

Abstract. We develop a general inverse Euler equation method to efficiently solve any multidimensional stochastic dynamic optimization problem with agents facing discrete-continuous choices and occasionally binding constraints. First, we provide a discrete time analogue to the Hamiltonian to (painlessly) recover the generalized necessary Euler equation. We then establish necessary and sufficient conditions to determine the existence of an Euler equation inverse, and the structure of the exogenous computational grid on which the inverse is well-defined. To handle applications with non-convexities generated by discrete choices, we finally present an off-the-shelf 'rooftop-cut' algorithm guaranteed to asymptotically recover the optimal policy function under standard economic assumptions. We demonstrate our approach using two workhorse applications in the literature, and document the computational speed and accuracy gains our method generates.

Key Words: discrete and continuous choices, non-convex optimization, Euler equation, dynamic programming, inverse optimization

JEL Classification: C13, C63, D91

[*] Corresponding author. School of Economics, University of New South Wales, Sydney 2052 Australia. Email: dobrescu@unsw.edu.au.

[†] School of Economics, University of New South Wales, Australia and ARC Center for Excellence in Population Ageing Research (CEPAR), Sydney 2052 Australia. Email: a.shanker@unsw.edu.au.

[‡] We thank Max Blesch, Chris Carroll, Mateo Velasquez-Giraldo, Greg Kaplan, Sebastian Gsell, Mike Keane, Anant Mathur, Olivia Mitchell, Adrian Monninger, Lucas Pahl, and John Stachurski for valuable discussions and comments. Research support from the Australian Research Council (ARC LP150100608) and ARC Centre of Excellence in Population Ageing Research (CE17010005) is gratefully acknowledged. This research was undertaken with the assistance of resources and services from the National Computational Infrastructure (NCI), which is supported by the Australian Government. The software implementing the RFC algorithm and the applications can be found here. All the proofs associated to the theoretical results are provided in the online appendix here.

1. Introduction

The prolonged focus on consumption and saving behavior, economic mobility, income and wealth inequality, social insurance, and redistributive policies has led economists to increasingly incorporate agent heterogeneity and behavioral frictions into dynamic decision-making models with uncertainty. Such models have been widely employed to help us understand, for instance (i) life-cycle wealth accumulation (French, 2005; Fagereng et al., 2017; Dobrescu et al., 2018), (ii) saving frictions (Kaplan and Violante, 2014; Berger and Vavra, 2015; Kaplan et al., 2020), (iii) labour choices (Attanasio et al., 2018; Iskhakov and Keane, 2021), (iv) housing dynamics (Cocco, 2005; Yogo, 2016; Fagereng et al., 2019) and mortgage refinancing effects on life-cycle asset allocation (Laibson et al., 2021), (v) risk of defaulting (Arellano, 2008; Arellano et al., 2016; Jang and Lee, 2023), (vi) firm investments with adjustment costs (Cooper, 2006; Khan and Thomas, 2008; Alfaro et al., 2024), as well as (vii) precautionary savings motives (Aiyagari, 1994; Carroll, 1997; Gourinchas and Parker, 2002), (viii) wealth accumulation with liquidity constraints (Deaton, 1991; Carroll, 1997; Dávila et al., 2012), (xi) distributional effects of business cycles (Krusell and Smith, 1998; Buera and Moll, 2015), and (x) policy transmission (Krueger et al., 2016; Kaplan et al., 2018; Beraja and Zorzi, 2023).

The challenges associated with solving and estimating these models are well known. Due to the curse of dimensionality (Rust, 1987), doing so is highly prohibitive using standard numerical methods. Even with the recent advances in computing power, applying the most novel computational methods proposed in the last few years (e.g., adaptive sparse grids - Brumm and Scheidegger (2017), polynomial chaos expansions - Pröhl (2023), machine learning - (Duarte et al., 2020; Fernández-Villaverde et al., 2023) to more interesting versions of these models remains a complex and computationally highly intensive endeavor. Several studies have recognized that significant speed and accuracy can be gained in standard settings by solving the Euler equation of the multidimensional dynamic stochastic optimization problem (Coleman, 1990; Reffett, 1996; Li and Stachurski, 2014). Additionally, methods that involve inverting the Euler equation (e.g., the endogenous grid method - EGM)[1] were even shown to eliminate the need for numerical methods altogether (Carroll, 2006).

However, studies (i)-(vi) above prominently feature discrete choices, while occasionally binding constraints are central in studies (vii)-(x). These elements lead to a breakdown of the standard convexity and smoothness assumptions required for Euler equation methods to work in a transparent and robust manner (Achdou et al., 2021). First, discrete choices introduce non-convexity, which can lead to multiple sub-optimal solutions to the Euler equation (Iskhakov et al., 2017). Second, with both discrete choices and occasionally binding constraints, policy functions may not be differentiable everywhere, precluding the use of standard envelope condition methods to derive the Euler equation (González-Sánchez and Hernández-Lerma, 2013). One must thus employ restrictive assumptions (i.e., boundedness, compactness) on the reward functions and feasibility correspondences (Rincón-Zapatero and Santos, 2009; Rendahl, 2015) that are generally violated in less stylized settings (Carroll, 2023). Third, when using methods that invert the Euler equation to

[1]Other methods that use Euler equations include Coleman-Reffett policy iteration (Coleman, 1990; Reffett, 1996; Li and Stachurski, 2014), the envelope condition method (Maliar and Maliar, 2013; Arellano et al., 2016), and deep learning methods that minimize the Euler equation error (Maliar et al., 2021).

reduce the numerical burden involved in solving multidimensional models, one does not know what conditions (that can be easily verified) are required for the inverse to be well-defined. Additionally, when occasionally binding constrains are also involved, there are no results to determine the optimal constraint choice implied by an inverse solution without going back to costly numerical optimization (Druedahl and Jørgensen, 2017). Finally, there are no results in general addressing any of these challenges for discrete time applications. Consequently, the application of Euler equation methods in dynamic stochastic modelling, while promising, has so far been stylized or ad hoc, and often incorporated alongside costly numerical optimization in more complex problems.

Our paper aims to close this gap. In particular, using recent advances in inverse optimization (Iyengar and Kang, 2005; Chan et al., 2023),[2] we derive a generalized necessary Euler equation, characterize its invertibility, and provide an efficient algorithm to recover the optimal policy function in the presence of multiple local optima.

In doing so, we see our contribution as threefold. First, as mentioned, we formalize the necessary recursive Euler equation, doing so for any *any* multidimensional dynamic stochastic optimization problems, including those with agents facing discrete choices and occasionally binding constraints. The approach we take is to characterize the Euler equation by introducing a discrete time analogue to the stochastic Hamiltonian - the 'S-function'. The S-function represents the change in the objective function value given a time-, state- and information-specific perturbation of the current period state. The S-function differentiation can then be defined in terms of real-valued calculus on the model primitives, and the Euler equation can be recovered without cumbersome envelope conditions or abstract functional derivatives. This is extremely beneficial in less stylized applications.

Second, we develop a general inverse Euler equation method to solve dynamic stochastic optimization problems that resolves all the challenges above. Recall that methods that invert the Euler equation reduce the need to find numerical solutions to dynamic optimization problems (Iyengar and Kang, 2005; Carroll, 2006). Our innovation is to define the inverse Euler equation on the joint space of end-of-period states (or 'post-states') *and* intratemporal Kuhn-Tucker multipliers of the constraints (i.e., the space of 'observable variables'), which allows us to robustly handle occasionally binding constraints. We then provide necessary and sufficient conditions for 'pure EGM', a situation where the Euler equation can always be inverted (analytically or numerically) on the space of observable variables. One fundamental insight of the results here is that the structure of the exogenous grid on which the inverse Euler equation is well-defined is solely determined by the state space dimension, even in regions where constraints bind. To use pure EGM, the number of post-states must be equal to the state space dimension, allowing us to formally define an inverse Euler equation that maps directly to the first order conditions (FOCs) of the S-function, and thus clearly identifies which constraints bind in each region of the exogenous grid.

[2]Inverse optimization is founded in geophysics (Sen and Stoffa, 2013) and has more recently gained tremendous traction in the AI literature, where inverse reinforcement learning has been used to recover parameters from observed actions. Up to our best knowledge, we are the first to formalise and deploy this theory as a formal method to solve dynamic stochastic optimization problems.

Obviously, in applications with more post-states than states, pure EGM cannot be applied (e.g., Berger and Vavra (2015), Kaplan et al. (2020)). For such situations, we provide the conditions on the policy function (i.e., local injectivity and continuity) guaranteeing that the Euler equation can be inverted from a reduced-dimensional subset (i.e., submanifold) of the observable space. Numerical root-finding can then be used to construct the exogenous grid such that our inverse Euler equation method can still bring significant computational efficiency gains. Note also that these results allow the inverse Euler equation to be robustly employed in any model (with or without discrete choices) where an analytical inverse to the Euler equation may not exist.

Third, we present a computationally efficient, accurate, and user-friendly algorithm to obtain the optimal policy functions for any multidimensional dynamic stochastic optimization problem with both discrete and continuous choices and occasional binding constraints. The algorithm, dubbed 'rooftop-cut' (or RFC), checks each solution point (i.e., each point of the endogenous grid) to see if the tangent to the future choice-specific value function at that point dominates neighboring points. If a neighboring point is dominated and moving to it induces a jump in the policy function, then this point is removed as sub-optimal. If a neighbouring point dominates the tangent, it is retained in the endogenous (solution) grid. Note here that RFC has the advantage of being able to recover the upper envelope of the value correspondence generated by the local solutions to the necessary Euler equation regardless of the interpolation method on the irregular multidimensional endogenous grid. It can also be easily programmed using vectorized (array) operations, making it compatible with high-performance computing infrastructure and programming languages.

Fourth, we provide pointwise asymptotic error bounds for our inverse Euler equation method both in the discrete-continuous case and for applications without discrete choices, under standard economic assumptions. These assumptions only relate to the Lipshitz continuity of the policy function,[3] and to the monotonicity of the policy function where it is continuous. This is particularly useful in simulation-based studies where the moments generated by the optimal policies computed via generalized inverse Euler equation and RFC (or EGM without discrete choices) become asymptotically accurate as the exogenous grid is refined.

Finally, we use two widely-used applications to illustrate the applicability of our method. Consider first a life-cycle model a' la Druedahl and Jørgensen (2017) in which agents facing unemployment risks decide how much to save in pensions and financial assets, and whether to retire or not. In this case, we show how the Euler equation derived using the S-function can be used to determine the optimal binding constraints given a point in the exogenous grid, without deriving separate policy functions for each constrained choice and without numerical loops to optimize over the constraint choices. With four possible combinations of binding constraints, RFC with Delaunay triangulation is (i) as fast as the original method by Druedahl and Jørgensen (2017), both methods being two orders of magnitude faster than value function iteration (VFI), and (ii) slightly more accurate, with gains coming from using first order information to 'delete' sub-optimal points. Adding just one

[3]The vast majority of economic applications involve bounded marginal propensities to consume and save, implying Lipshitz continuity. While a key RFC advantage is that it does not require monotonicity of the policy function, the agents problem holding future choices fixed is a concave problem with standard monotonicity (White, 2015).

extra single constraint (e.g., a cap on pension contributions) leads to 50% increase in the number of possible binding constraint combinations, and so 50% increase in the computation time using the original method. On the other hand, using our inversion results to determine the optimal constraint from the exogenous grid and RFC leaves total computation time unchanged. Next, we do the same to examine a portfolio allocation problem with housing and financial assets, where previous discrete-continuous Euler equation methods fail due to (i) non-monotonic policy functions, and (ii) an irregular exogenous grid that arises because the Euler equation is not analytically invertible. Somewhat unsurprisingly, we find RFC to be again two orders of magnitude faster and more accurate than standard VFI. Compared, however, to the most efficient prior attempts to solve this type of problems, which use an EGM step nested within numerical optimization (Druedahl, 2021), RFC gains up to an order of magnitude better accuracy and 25% higher speed.

Our paper advances considerably the latest dynamic programming methods. First, in relation to the theoretical foundation of Euler equations (Sorger, 2015; Rincón-Zapatero and Santos, 2009; Li and Stachurski, 2014; Rendahl, 2015; Ma et al., 2022; Stachurski, 2022), we are the first to provide the necessary and sufficient conditions for the generalized Euler equation to accommodate occasionally binding constraints, discrete choices, unbounded rewards, and non-compact feasibility correspondences. Second, while the underlying intuition behind inverting the Euler equation and EGM as an inverse problem was introduced in a special case by Carroll (2006) and has spawned a significant literature (Barillas and Fernandez-Villaverde, 2007; White, 2015; Iskhakov, 2015; Ludwig and Schön, 2018; Lujan, 2023), we are the first to develop a formal theory of inverse optimization to solve discrete-continuous dynamic stochastic problems even when facing the challenges detailed above. Specifically, we provide (i) verifiable error bounds, (ii) necessary and sufficient conditions for EGM to be well-defined (with or without discrete choices), and (iii) the conditions that characterize the structure of the exogenous grids. Third, in terms of the EGM implementation in discrete-continuous choice models (Fella, 2014; Iskhakov et al., 2017; Druedahl and Jørgensen, 2017; Druedahl, 2021), our RFC algorithm is the first to (i) not require regularity of the exogenous grid or monotonicity of the optimal policy, (ii) be asymptotically guaranteed to approximate the optimal solution, and (iii) allow high-dimensional discrete-continuous models to exploit the massive parallelism of modern high performance computing infrastructure (e.g., GPUs). Up to our best knowledge, only Dobrescu and Shanker (2023) attempts to recover the upper envelope of the value correspondence for discrete-continuous EGM when the policy function is non-monotone. Unlike RFC, which works in multiple dimensions and uses the value function gradient, the FUES method by Dobrescu and Shanker (2023) (i) uses secants to eliminate neighbouring points, (ii) can only be applied to one-dimensional problems, and importantly, (iii) does not address any of the theoretical challenges listed above. Finally, our paper relates to the broader optimization literature that seeks to address the issues associated with numerically solving richer, more complex dynamic models. For instance, Brumm and Scheidegger (2017) tackles the high-dimensionality of their model by developing a method to refine sparse grids, Achdou et al. (2021) suggests continuous time modelling, and Maliar et al. (2021) and Auclert et al. (2021) propose ways to arrive at and approximate the stationary policies. Our work complements these approaches by developing a method that focuses on the within period solution in (stationary or non-stationary) discrete time models. Moreover,

it can accurately handle non-convexities arising from discrete choices, and also allows models to efficiently scale with the dimension of the state and the number of constraint choices. This makes it applicable to all multidimensional dynamic stochastic optimization problems in which non-smooth, non-monotone and discontinuous policy functions lead to computational challenges. Consequently, while our results support a more direct implementation of Euler equation methods in stylized applications (Aiyagari, 1994; Huggett, 1996; Krusell and Smith, 1998; Fella, 2014; Iskhakov et al., 2017; Druedahl and Jørgensen, 2017), they also allow more interesting, complex multidimensional models – such as heterogeneous agents models with household formation and labour choices (Kekre, 2022; Bardoćzy, 2022), structural life-cycle models with consumer credit (Best et al., 2019; Crawford and O'Dea, 2020; Dobrescu et al., 2022) or dynamic human capital accumulation models (Hai and Heckman, 2019; Dobrescu et al., 2024) – to be solved and estimated efficiently.

The paper proceeds as follows. Section 2 introduces the setup of a general dynamic programming problem, and discusses the challenges to the Euler equation identified in the literature. Section 3 introduces the S-function and proves the necessary FOCs. Section 4 formalizes the inverse dynamic optimization problem, provides necessary and sufficient conditions for the invertibility of the Euler equations, and introduces the RFC algorithm with its convergence properties. Section 5 presents two applications of the theory, together with the analysis of the accuracy and speed gains from our method compared to previous ones. Section 6 concludes.

2. General setup and preliminary considerations

2.1. **Notation.** To ease readability, in what follows we will use italic to denote variables, roman fonts for functions, and capital letters for spaces - e.g., at time t, y_t is a variable in the post-decision state (or 'post-state') space Y_t with $y_t \in Y_t$, and y_t is the post-state policy function.[4] Additionally, we use (i) bold letters with a $\vec{}$ superscript to denote a sequence of variables across time - e.g., $\vec{\boldsymbol{y}}_t = \{y_t, y_{t+1}, \ldots, y_T\}$ with T the terminal period of the dynamic programming problem, and (ii) capital calligraphic letters for a sequence of grid points labelled with superscript $^{\#}$ - e.g., $\mathcal{Y}_t = \left\{y^{\#}_{t,0}, \ldots, y^{\#}_{t,N}\right\}$ is a grid of N post-state points at time t with $\mathcal{Y}_t \subset Y_t$.

For clarity, we also note the following mathematical conventions used below. We use $\|\cdot\|$ to denote to the Euclidean norm. For a set $S \subset \mathbb{R}^n$, S^{o} refers to its interior, and for $x \in \mathbb{R}^n$, $\mathbb{B}_\epsilon(x)$ refers to the ϵ-ball about x. For an $m \times n$ matrix $\mathbf{A}$ and $n \times p$ matrix $\mathbf{B}$, $\mathbf{AB}$ denotes the matrix product. When $\mathbf{B}$ is also an $m \times n$ matrix, $\mathbf{A} \circ \mathbf{B}$ will denote the Hadamard or pointwise product. For two euclidean column vectors a and b, we use $a \cdot b$ to denote the inner-product. For a function $\mathrm{f}\colon \mathbb{R}^n \times \mathbb{R}^k \to \mathbb{R}^m$, partial derivatives and the Jacobian with respect to the argument x are denoted using $\partial_x \mathrm{f}(x, y)$. Moreover, letting $\mathrm{f} = (\mathrm{f}_1, \ldots, \mathrm{f}_m)$, the Jacobian can be written as $\partial_x \mathrm{f}(x, y) = [\nabla_x \mathrm{f}_1(x, y), \ldots, \nabla_x \mathrm{f}_m(x, y)]^\top$, where $\nabla_x \mathrm{f}_1(x, y)$ denotes gradient column vectors and $\top$ denotes the matrix transpose.

[4]To further streamline exposition, we will use italic to denote both (i) a random variable that realizes in the state and post-state space ('history contingent plans' - see Hernandez-Lerma and Lasserre (2012)), and (ii) the realized value of a random variable, as a state or post-state, at a given time - a distinction that is important when we prove our Euler equation results. A formal mathematical treatment is given in the online appendix, where we set up a stochastic sequence problem in a Hilbert space.

Finally, (i) $\pi_Y \colon X \times Y \to Y$ denotes a projection operator defined by the evaluation $\pi_Y(x, y) = y$, and (ii) fixing $x^\star \in X$, we use $\mathrm{em}_Y \colon Y \to X \times Y$ to denote the embedding $y \mapsto (x^\star, y) = \mathrm{em}_Y(y)$.

2.2. **The general dynamic optimization problem setup.** We start by setting up a generic reduced form dynamic optimization problem[5] that is consistent with the recent literature (Hernandez-Lerma and Lasserre, 2012; Hull, 2015; Ma et al., 2022; Sargent and Stachurski, 2023), but also explicitly incorporates discrete actions and states (Druedahl and Jørgensen, 2017).

Let t index time, and assume $t \in \{0, \dots, T\}$, where $T \in \mathbb{N} \cup \{\infty\}$. For each t, the dynamic programming problem consists of the following:

(1) A state space $X_t = W_t \times Z_t \times M_t$, where:
   (i) W_t is an exogenous shock space, with $W_t \subset \mathbb{R}^{N_W}$,
   (ii) Z_t is a discrete state space, with $Z_t \subset \mathbb{R}^{N_Z}$, and
   (iii) M_t is a continuous state space, with $M_t \subset \mathbb{R}_+^{N_M}$.

(2) A W_t-valued stochastic recursive sequence $\{w_t\}_{t=0}^T$ of shocks, with a transition kernel F_t^w.[6]

(3) An action space $D_t \times Y_t$, where:
   (i) D_t is a discrete choice space, with $D_t \subset \mathbb{N}^{N_D}$, and
   (ii) Y_t is a continuous post-state space, with $Y_t \subset \mathbb{R}^{N_Y}$.

(4) A feasibility correspondence Γ_t, with $\Gamma_t \colon X_t \rightrightarrows D_t \times Y_t$, where $(d_t, y_t) \in \Gamma_t(x_t)$ if and only if $\mathrm{g}_t(w_t, z_t, m_t, d_t, y_t) \geq 0$ for a concave measurable function g_t, with $\mathrm{g}_t(w_t, z_t, \cdot, d_t, \cdot) \colon \mathbb{R}^{N_M} \times \mathbb{R}^{N_Y} \to \mathbb{R}^{N_g}$ for each $(w_t, z_t, d_t) \in W_t \times Z_t \times D_t$.

(5) A concave measurable reward function u_t, with $\mathrm{u}_t \colon \mathrm{Gr}\Gamma_t \to \mathbb{R} \cup \{-\infty\}$, where we write $\mathrm{u}_t(w_t, z_t, m_t, d_t, y_t)$ as the evaluation of u_t.

(6) A transition kernel F_t^m for the continuous state, with $\mathrm{F}_t^m \colon D_t \times Y_t \times W_{t+1} \to M_{t+1}$, and a discrete transition kernel F_t^d, with $\mathrm{F}_t^d \colon D_t \times W_{t+1} \to Z_{t+1}$.

Each period, the agent observes a state x_t, with $x_t \in X_t$, and responds with two actions: a feasible discrete choice $d_t \in D$, and a continuous post-state $y_t \in Y_t$ such that $(d_t, y_t) \in \Gamma_t(x_t)$. The agent obtains a reward $\mathrm{u}_t(w_t, z_t, m_t, d_t, y_t)$ and moves to the next period random state x_{t+1}, where $x_{t+1} = (w_{t+1}, z_{t+1}, m_{t+1})$ and

$$x_{t+1} = \mathrm{F}_t(d_t, y_t, w_{t+1}) \tag{1}$$

with F_t denoting the tuple $(\mathrm{F}_t^w, \mathrm{F}_t^d, \mathrm{F}_t^m)$.

The agent solves for a sequence of measurable policy functions $\{\mathrm{d}_t, \mathrm{y}_t\}_{t=0}^T$, where $\mathrm{d}_t \colon X_t \to D_t$ and $\mathrm{y}_t \colon X_t \to Y_t$ for each t. Given the initial state $x_0 \in X_0$, the value function $\mathrm{v}_0 : X_0 \to \mathbb{R} \cup \{-\infty\}$

[5]Specifying the problem in reduced form without controls (Sorger, 2015) is without loss of generality.

[6]Without loss of generality, we can assume (i) $w_{t+1} = \mathrm{F}_t^w(w_t, \eta_{t+1})$ for a measurable function F_t^w, where $\{\eta_t\}_{t=0}^T$ is a sequence of random variables defined on a common probability space $(\Omega, \Sigma, \mathbb{P})$, and (ii) w_0 is degenerate. Note that a stochastic recursive sequence (SRS) is more general than a Markov process (Borovkov, 2013; Stachurski, 2022).

becomes

$$\textbf{(DP)} \qquad \mathrm{v}_0(x_0) = \sup_{\{\mathrm{d}_t,\mathrm{y}_t\}_{t=0}^T} \mathbb{E}_{x_0} \sum_{t=0}^{T} \mathrm{u}_t(w_t, z_t, m_t, \mathrm{d}_t(x_t), \mathrm{y}_t(x_t))$$

such that (1) holds with $y_t = \mathrm{y}_t(x_t)$ and $d_t = \mathrm{d}_t(x_t)$ for each t, and $(\mathrm{d}_t(x_t), \mathrm{y}_t(x_t)) \in \Gamma_t(x_t)$ for each t and x_t – i.e., such a sequence $\{\mathrm{d}_t, \mathrm{y}_t\}_{t=0}^T$ of policy functions is feasible. The conditional expectation operator $\mathbb{E}_{x_0}$ is conditional on the time $t = 0$ realization of the state. To maintain generality, we do not specify a particular structure of time discounting; following (Cosar and Green, 2014), u_t can be interpreted as a payoff discounted to $t = 0$.

Since our aim is to provide a general method to characterize and solve (**DP**), we assume for brevity that a solution to this problem exists. In practice, solution existence can be verified using the recent methods in the literature (Feinberg et al., 2012; Shanker, 2017; Ma et al., 2022; Carroll, 2023).

Assumption 1. *There exists a sequence of feasible sequence of measurable policy functions* $\{\mathrm{d}_t, \mathrm{y}_t\}_{t=0}^T$ *such that* $\mathrm{v}_0 \colon X_0 \to \mathbb{R}$ *and*

$$\mathrm{v}_0(x_0) = \mathbb{E}_{x_0} \sum_{t=0}^{T} \mathrm{u}_t(w_t, z_t, m_t, \mathrm{d}_t(x_t), \mathrm{y}_t(x_t)) < \infty, \qquad x_0 \in X_0 \tag{2}$$

Under Assumption 1, the Bellman equation for each v_t, conditional on time t information, becomes

$$\textbf{(BE)} \qquad \mathrm{v}_t(x_t) = \max_{d_t, y_t \in \Gamma_t(x_t)} \left\{ \mathrm{u}_t(w_t, z_t, m_t, d_t, y_t) + \mathbb{E}_{x_t} \mathrm{v}_{t+1}(x_{t+1}) \right\}, \qquad x_t \in X_t$$

such that (1) holds. We can also write a current period discrete choice ('current discrete choice')-specific Bellman equation as

$$\mathrm{v}_{d_t,t}(x_t) = \max_{y_t \in \Gamma_{d_t,t}(x_t)} \left\{ \mathrm{u}_t(w_t, z_t, m_t, d_t, y_t) + \mathbb{E}_{x_t} \mathrm{v}_{t+1}(x_{t+1}) \right\}, \qquad x_t \in X_t \tag{3}$$

where $\Gamma_{d_t,t}$ denotes the set $\{y_t \,|\, d_t, y_t \in \Gamma_t(x_t)\}$, and we let $\mathrm{y}_{d_t,t}$ denote the current discrete choice-specific policy function.

While we characterize the Euler equation of the problem in Section 3, the following notation will aid the discussion below:

Remark 1. *For each* t*, a sufficient and necessary Euler equation for the maximization problem in* (3) *is a function* $\mathbf{E}_t \colon \mathbb{R}^{N_Y} \times \mathbb{R}^{N_g} \times \mathbb{R}^{N_M} \to \mathbb{R}^{N_Y} \times \mathbb{R}^{N_g}$ *such that* $\mathbf{E}_t(y_t, \mu_t \,|\, m_t) = 0$ *if and only if* y_t *solves* (3) *given the state* m_t *and* (w_t, z_t, d_t) *and multiplier* μ_t*.*

2.2.1. *Fixed variables and active state space.* The post-state policy functions are usually computed in applications given (i) a realization of an exogenous shock, and (ii) the values of the discrete state and of the current discrete choice. It will thus be useful to collect these 'fixed' variables in a tuple ξ_t, where $\xi_t \colon = (w_t, z_t, d_t)$.

Furthermore, note that during computation, the dimensionality of the continuous state space can often be reduced.[7] To formalize the dimensionality reduction in our general setting, we consider the problem to have an 'active state representation' if there exists (i) $\bar{M}_t \subset \mathbb{R}^{N_M}$ such that $\dim(\bar{M}_t) =: N_{\bar{M}} < N_M$, and (ii) continuous selection functions $\phi_t \colon M_t \to \bar{M}_t$ and $\bar{\mathrm{y}}_t(\xi_t, \cdot) \colon \bar{M}_t \to Y_t$ such that if $\mathrm{y}_{d_t,t}$ is an optimal policy then $\mathrm{y}_{d_t,t}(x_t) = \bar{\mathrm{y}}_t(\xi_t, \phi_t(m_t))$ for all x_t and d_t. In what follows, when the fixed variables ξ_t are given, we will abbreviate $\bar{\mathrm{y}}_t(\xi_t, \bar{m}_t)$ to $\bar{\mathrm{y}}_t(\bar{m}_t)$, where the dependence of $\bar{\mathrm{y}}_t$ on ξ_t is implicit. We can similarly define the evaluation of the reward function and constraints on the active state space as $\bar{\mathrm{u}}_t(\phi_t(m_t), y_t)$ and $\bar{\mathrm{g}}_t(\phi_t(m_t), y_t)$, respectively.

2.3. **Euler equation challenges.** Before we turn to characterizing the Euler equation and its arguments, we detail the three challenges that arise when computing the solution to the problem above using an Euler equation.

2.3.1. *Non-concavity and sufficiency of the Euler equation.* We start our discussion of computational challenges to Euler equations by formally explaining the reasons why the value function may not be concave in the presence of discrete choices. This formalization will also play a key role in the algorithm we present to remove sub-optimal points.

To begin, fix x_t and let $\vec{\boldsymbol{d}}_t = \{d_j, \ldots, d_T\}$ denote a stochastic sequence of discrete choices starting at time t and ending at time T, to which we refer to as 'future discrete choices'. In particular, let $\{\mathrm{d}_j, \mathrm{y}_j\}_{j=t}^T$ be a sequence of discrete choice and post-state policy functions. Define the discrete choices and states generated under these policies as[8]

$$d_j = \mathrm{d}_j(x_j), \qquad x_j = \mathrm{F}(d_j, \mathrm{y}_j(x_j), w_{j+1}) \tag{4}$$

Consider the future choice-specific dynamic programming problem

$$\mathrm{v}_t^{\vec{\boldsymbol{d}}_t}(w_t, z_t, m_t) \colon = \max_{\{\mathrm{y}_j\}_{j=t}^T} \mathbb{E}_{x_0} \sum_{j=0}^{T} \mathrm{u}_j(w_j, z_j, m_j, d_j, \mathrm{y}_j(x_j)), \tag{**CS-DP**}$$

such that (1) holds. Since the stochastic sequence of future discrete choices $\vec{\boldsymbol{d}}_t$ remains fixed for each t, the problem becomes a standard concave dynamic optimization problem. Moreover, $\mathrm{v}_t^{\vec{\boldsymbol{d}}_t}(w_t, z_t, \cdot)$ will be a concave function. Next, let $\Gamma_{\mathrm{D},t}^T$ denote the correspondence defined on the X_t mapping to feasible future discrete choices starting at t, with[9]

$$\Gamma_{\mathrm{D},t}^T(x) \colon = \Big\{ \vec{\boldsymbol{d}}_t \in \bigtimes_t^T D_t \,\Big|\, d_j, y_j \in \Gamma_j(x_j), \; x_{j+1} = \mathrm{F}_j(d_j, y_j, w_{j+1}), x_t = x, j = t, \ldots, T \Big\} \tag{5}$$

[7]See for instance Fella (2014), where in a model with two wealth states (i.e., financial assets and housing), one overall wealth state becomes sufficient to compute the optimal policy for those who adjust housing stock.

[8]The sequence $\{d_j, x_j\}_{j=t}^T$ will be progressively measurable with respect to the filtration generated by the random variables $\{w_j\}_{j=t}^T$, with a realization of w_t fixed.

[9]The feasible set of sequences of future discrete choices should be understood to contain sequences of random variables, while set relations and equalities in the definition of $\Gamma_{\mathrm{D},t}^T$ hold $\mathbb{P}$ almost everywhere.

If $\vec{\boldsymbol{d}}_t \in \Gamma^T_{\mathrm{D},t}(x_t)$, we will simply say $\vec{\boldsymbol{d}}_t$ is feasible given x_t. The Bellman equation for our original problem (**BE**) can now be written as

$$\textbf{(BE-2)} \qquad \begin{aligned} \mathrm{v}_t(x_t) &= \max_{d_t, y_t \in \Gamma_t(x_t)} \left\{ \mathrm{u}_t(w_t, z_t, m_t, d_t, y_t) + \max_{\vec{\boldsymbol{d}}_{t+1}} \left\{ \mathbb{E}_{x_t} \mathrm{v}^{\vec{\boldsymbol{d}}_{t+1}}_{t+1}(w_{t+1}, z_{t+1}, m_{t+1}) \right\} \right\} \\ &= \max_{d_t, y_t \in \Gamma_t(x_t)} \max_{\vec{\boldsymbol{d}}_{t+1}} \Big\{ \underbrace{\mathrm{u}_t(w_t, z_t, m_t, d_t, y_t) + \mathbb{E}_{x_t} \mathrm{v}^{\vec{\boldsymbol{d}}_{t+1}}_{t+1}(w_{t+1}, m_{t+1})}_{=: \mathrm{Q}^{\vec{\boldsymbol{d}}_{t+1}}_t(x_t, d_t, y_t)} \Big\} \end{aligned}$$

such that $\vec{\boldsymbol{d}}_{t+1}$ is feasible given x_{t+1}, and (1) holds. Even if we hold d_t and d_{t+1} fixed, the next period value function v_{t+1} will not be concave in the continuous state. This is because the max operator over the non-convex set $\Gamma^T_{\mathrm{D},t+1}(x_{t+1})$ does not commute concavity, and v_{t+1} is the upper envelope over a sequence of feasible future discrete choices. Figure 1 illustrates this situation by showing v_t as the upper envelope of the concave functions $\mathrm{v}^{\vec{\boldsymbol{d}}_t}_t(w_t, z_t, \cdot)$, where each of these concave functions is a value function conditional on a *sequence* of future discrete choices. Thus, even with d_t held fixed, the optimization problem given by (3) remains non-concave. As such,

$$\mathrm{v}_{d_t,t}(x_t) = \max_{y_t \in \Gamma_t(x_t)} \mathrm{Q}_t(x_t, d_t, y_t), \tag{6}$$

where

$$\textbf{(Q)} \qquad \mathrm{Q}_t(x_t, d_t, y_t) = \max_{\vec{\boldsymbol{d}}_{t+1}} \mathrm{Q}^{\vec{\boldsymbol{d}}_{t+1}}_t(x_t, d_t, y_t),$$

will not be concave. By controlling y_t in the Q function, we implicitly control the stochastic sequence of future discrete choices, leading to secondary kinks in the value function and discontinuous jumps in the policy function.

The FOCs of the current choice-specific problem are thus not sufficient to characterize the optimal policy function since they do not select the optimal future sequence of discrete choices - or the upper envelope - in Figure 1. As such, the Euler equation will have multiple roots, and there will be multiple local optima that will satisfy $\mathbf{E}_t(y_t, \mu_t \,|\, m_t) = 0$. Importantly, when using an inverse Euler equation method such as EGM, we do not have access to all the possible roots for any given continuous state m_t – we only know the tuples $(m_t, y_t, v^{\vec{\boldsymbol{d}}_{t+1}}_t)$, where $\vec{\boldsymbol{d}}_{t+1}$ is optimal at $t+1$ if y_t is the end-of-period t post-state; we thus cannot compare the value function evaluated at each of these multiple roots to determine which $\vec{\boldsymbol{d}}_{t+1}$ is optimal given m_t.

The recent literature has proposed methods to determine the upper envelope of the future choice-specific value functions generated by EGM, which invert the necessary FOCs (Fella, 2014; Druedahl and Jørgensen, 2017; Iskhakov et al., 2017). Two key limitations continue, however, to persist, namely (i) the inability of these algorithms to solve problems where both exogenous and endogenous grid points may be irregular or non-monotone (see application 5.2.3 below, that cannot be solved using existing methods), and (ii) the lack of assurance (asymptotic or otherwise) that these methods are accurate for an arbitrary problem. Iskhakov et al. (2017) introduces a method contingent on the monotonicity of the optimal policy that only accommodates 'upward' policy function jumps. This approach is demonstrated for a specific model, within a one-dimensional setting, and does not

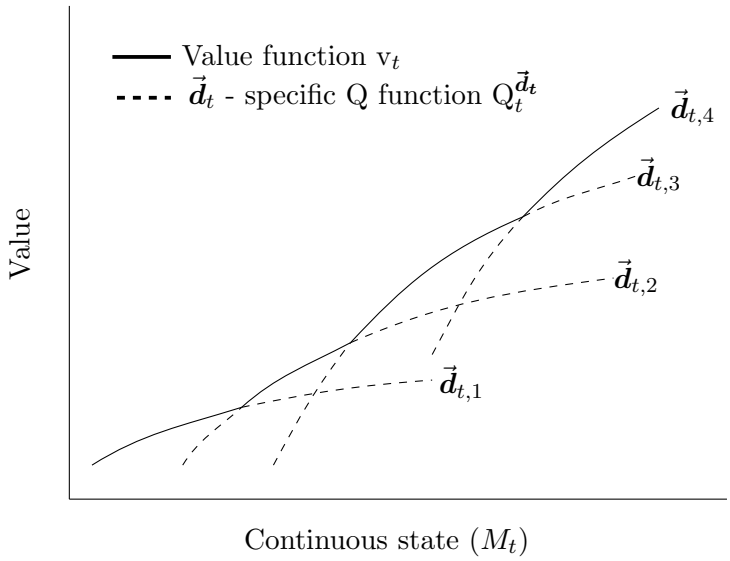

Figure 1. As a function of the continuous state, the time t value function v_t is the upper envelope of concave functions, where each concave function is a value function conditional on a stochastic *sequence* of future discrete choices; the subscript i on $\vec{d}_{t,i}$ indicates distinct stochastic sequences of future discrete choices

provide a theoretical indication of its precision or convergence. It also requires the exogenous grid to be regular, and only applies to cases where one can verify that the policy function is monotone, and the endogenous grid consists of clearly discernible monotone and connected segments.[10] In contrast, Druedahl and Jørgensen (2017) offers a multidimensional algorithm that generates local triangulations on the endogenous grid by identifying triangles within the exogenous grid. The authors note that the points retrieved by their method become asymptotically dense in the optimal grid, but do not establish error bounds for approximations of the policy function. Additionally, their method cannot be applied when the exogenous grid is irregular, and it is also tied to a particular interpolation and triangulation method (i.e., local triangulation using simplices on the exogenous grid). Doing so, however, precludes using standard, off-the-shelf interpolation methods such as Gaussian process regressions (Lujan, 2023) and Delaunay triangulations (Chen and Xu, 2004)).

2.3.2. *Non-differentiability and necessity of Euler equation.* Figure 1 shows how the value function cannot be differentiable at the intersection points. Specifically, $\mathrm{v}_t(x_t) = \mathrm{u}_t(w_t, z_t, m_t, d_t, \mathrm{y}_t(m_t)) + \mathbb{E}_{x_t}\mathrm{v}_t(x_{t+1})$ and $x_{t+1} = \mathrm{F}_t(d_t, \mathrm{y}_t(m_t), w_{t+1})$, where y_t denotes the optimal policy function. If y_t exhibits a jump discontinuity due to a secondary kink at a given $\hat{m}_t$, then $\partial_m \mathrm{v}_t$ will be undefined at $\hat{m}_t$ because the left-hand side (LHS) and right-hand side (RHS) derivatives will not match (Iskhakov, 2015). Although Clausen and Strub (2020) characterize differentiability at locations

[10]In models of non-durable stock accumulation with fixed adjustment costs, policy functions are not monotone and the exogenous grid is itself a subset of a lower-dimensional manifold of the post-state space, leading to irregularly spaced points; Section 5.2.3 elaborates. Another example of a method that requires monotonicity is Fella (2014).

other than the kink points,[11] the implications for the Euler equation everywhere across the state space remain unexplored. Their method also requires analytically finding support functions, which may become very cumbersome in complex applications.

Differentiability of the value function has been challenging even in the absence of discrete choices. In models with occasionally binding constraints, y_t will not be differentiable, and the standard envelope condition approach to derive the Euler equation will fail if optimal policies are not all in the interior of the feasible set. While progress has been made to characterize Euler equations in the presence of occasionally binding constraints, existing results require compact feasibility correspondences and, at the same time, do not allow the reward function to reach $-\infty$ (Rincón-Zapatero and Santos, 2009; Rendahl, 2015; Marimon and Werner, 2021). As a result, the existing results end up not accommodating quite a wide range of realistic reward functions. In particular, if feasibility correspondences are to be compact, then constant relative risk aversion (CRRA) utility functions (i.e., with CRRA parameter above 1) in income fluctuation models, for instance, would require unbounded utility values that can reach $-\infty$ (Carroll, 2023). While Li and Stachurski (2014) and Ma et al. (2022) derive the Euler equation without such restrictions,[12], they only (i) focus on specific applications, and also (ii) assume bounded marginal utility and a strictly positive lower bound on earnings shocks. Finally, these approaches cannot apply to models with a naturally arising liquidity constraint, such as widely-used models with unemployment risk (Carroll, 2023).

All in all, a general 'off-the-shelf' theory to derive the Euler equation using standard real-valued calculus in the presence of discrete choices, multiple occasionally binding constraints, and unbounded reward functions has so far remained elusive.

2.3.3. *Constraints and invertibility of the Euler equation.* When using the Euler equation inverse to compute a solution, we solve $m_t \mapsto \mathbf{E}_t(y_t, \mu_t \,|\, m_t) = 0$ for m_t over an exogenous grid of y_t points. In this case, there is no formal theory of how to set up an exogenous grid such that the inverse of the Euler equation satisfying the optimal constraint choice is well-defined. The answer to this question determines how to construct the exogenous grid and the set of constraints that bind given an inverse solution. Iskhakov (2015) gives conditions for when an analytical inverse of the Euler equation exists on the post-state space for problems without constraints. While Druedahl and Jørgensen (2017) points out that the policy functions must be an injection, it does not provide specific conditions that determine the structure of the exogenous grid on which invertibility holds. To deal with constraints, the authors suggest evaluating the policy function using EGM for each possible constraint combination. The optimal policy function is then determined by an 'outer loop' that evaluates the value function on the state space for each constraint, and numerically chooses the optimal constraint. However, this outer loop leads to an unnecessary computational step that becomes costly in practical high-dimensional applications - such as Dobrescu et al. (2022) for instance. As we show in Section 4.1.1, the Euler equation sharply characterizes the exogenous grid

[11]Clausen and Strub (2020) prove a result indicating differentiability of the value function away from kink points, but under the assumption that the continuous choice is in the interior of the feasibility correspondence. Interiority is violated by many models, including our second application in Section 5 where a subset of the occasionally binding constraints actually end up binding (see Rincón-Zapatero and Santos (2009) and also Remark 5).

[12]See also Dávila et al. (2012) and Cao (2020)

on which an inverse exists, and the optimal constraints that bind given the inverse solution. This allows us to avoid any additional upper envelope loops by inverting only from the image of the policy function optimized over the constraint choice.

Finally, there are cases when an Euler equation inverse does not exist on the full post-state space but it may exist on a lower-dimensional subspace. In these instances, we will show that our inverse method can still be applied to gain computational efficiency and accuracy as in application 5.2.3.

3. The Generalized Euler Equation

We now turn to our first main contribution and address the non-differentiability challenge identified above. After providing the general conditions required to prove the necessity of Euler equations, we introduce an S-function that can be used to easily derive FOCs even in the presence of discrete choices, occasionally binding constraints, and non-differentiability of the value function. We also show that a saddle point to the S-function is a sufficient and necessary condition for optimality given a stochastic sequence of future discrete choices, and then use the saddle point of the S-function to characterize Euler equations.

3.1. Main necessary and sufficient conditions.

For the following assumptions, consider the setting of Assumption 1, and let $\{\mathrm{d}_t, \mathrm{y}_t\}_{t=0}^{T}$ be an optimal sequence of policy functions.

Assumption (D.1) For every $x_t \in X_t$ and $d_t \in D_t$, the function $\mathrm{u}_t(w_t, z_t, \cdot, d_t, \cdot)$ is continuously differentiable on $\mathbb{B}_\epsilon(m_t, y_t)$ for some $\epsilon > 0$ and $y_t = \mathrm{y}_t(x_t)$.

Assumption (D.2) For every $(w_t, z_t, d_t) \in W_t \times Z_t \times D_t$, the functions $\mathrm{g}_t(w_t, z_t, \cdot, d_t, \cdot)$ and $\mathrm{F}_t^m(d_t, \cdot, w_{t+1})$ are affine.

Assumption (D.3) For every $(w_t, z_t, m_t, d_t) \in W_t \times Z_t \times M_t \times D_t$, the Slater condition holds. That is, the set $\{y \,|\, \mathrm{g}_t(w_t, z_t, m_t, d_t, y) > 0, \mathrm{g}_t(w_{t+1}, z_{t+1}, m', d_{t+1}, y_{t+1}) > 0\}$ is non-empty, where $m' = \mathrm{F}^m(d_t, y, w_{t+1})$ and $y_{t+1} = \mathrm{y}_{t+1}(m_{t+1})$, $m_{t+1} = \mathrm{F}^m(d_t, \mathrm{y}_t(m_t), w_{t+1})$.

Assumptions D.1 - D.3 are unrestrictive (see discussion in Rincón-Zapatero and Santos (2009)). However, as mentioned above, our problem definition does not require that $\mathrm{u} > -\infty$ or that Γ_t is compact-valued, and we do not impose a strictly positive lower bound on the marginal reward (i.e., utility) or value of the shocks. Importantly, we also allow for the presence of discrete choices.

To derive the necessary and sufficient FOCs, we consider instantaneous time t values of multipliers, which we define as the functions $\mu_t \colon X_t \to \mathbb{R}^{N_g}$ and $\Lambda_t \colon X_t \to \mathbb{R}^{N_M}$, and refer to their evaluation as 'constraint multipliers' and 'shadow values of the state', respectively. At the optimum, the constraint multipliers, evaluated at the current state, represent the marginal value of relaxing each inequality constraint. In turn, the shadow values of the state indicate the marginal value of increasing each state variable at the start of time t.

Fix $x_t \in X_t$, the discrete choice function d_t, the post-state policy function y_t, and a next period state shadow value function Λ_{t+1}. The S-function at time t is defined by

$$(\mathbf{S}) \quad \mathbf{S}_t\left(m, y, \mu, \lambda \,|\, x_t, \mathbf{\Xi}_t\right) : = \mathrm{u}_t(w_t, z_t, m, d_t, y) + \mathbb{E}_{x_t}\Lambda_{t+1}(x_{t+1}) \cdot \mathrm{F}_t^m(d_t, y, w_{t+1}) - \lambda \cdot m + \mu \cdot \mathrm{g}_t(w_t, z_t, m, d_t, y)$$

where $m \in M_t, y \in Y_t, \mu \in \mathbb{R}^{N_g}, \lambda \in \mathbb{R}^{N_M}$. To ease the notation, $\mathbf{\Xi}_t$ denotes the tuple of functions $(\mathrm{d}_t, \mathrm{y}_t, \Lambda_{t+1})$ and $m_{t+1} = \mathrm{F}_t^m(d_t, \mathrm{y}_t(x_t),\ w_{t+1})$, $z_{t+1} = \mathrm{F}_t^d(d_t, w_{t+1})$, $w_{t+1} = \mathrm{F}_t^w(w_t, \eta_{t+1})$, $x_{t+1} = (w_{t+1}, m_{t+1}, w_{t+1})$ and $d_t = \mathrm{d}_t(x_t)$.

Analogous to a discrete time Hamiltonian, the S-function represents an incremental value of the objective function as a function of the state and post-state. In a stochastic discrete time setting, however, arguments for the Hamiltonian become infinite-dimensional objects (Bewley, 1972; Dechert, 1982). Our innovation is to represent the multipliers, shadow value and incremental value as *functions* of the real-valued current state *holding expectations over the future fixed.* The formulation avoids differentiating the value function, and at the same time avoids the use of abstract derivatives to compute the Euler equation. An immediate implication of using the S-function to derive the Euler equation is that it sharply characterizes the post-state and multiplier space in which constrained solutions exist (see Theorem 2 in the next section).

Our first main result tells us that if there exists a sequence of shadow value functions, non-negative constraint multipliers and policy functions such that m_t, $\mathrm{y}_t(x_t)$, $\mu_t(x_t)$ and $\Lambda_t(x_t)$ are a saddle point of the S-function in the sense that

$$\partial_m \mathbf{S}_t(m_t, \mathrm{y}_t(x_t), \mu_t(x_t), \lambda_t(x_t) \,|\, x_t, \mathbf{\Xi}_t) = 0 \tag{7}$$

$$\partial_y \mathbf{S}_t(m_t, \mathrm{y}_t(x_t), \mu_t(x_t), \lambda_t(x_t) \,|\, x_t, \mathbf{\Xi}_t) = 0 \tag{8}$$

$$\mathrm{g}_t(w_t, z_t, m, d_t, \mathrm{y}_t(x_t)) \geq 0 \tag{9}$$

$$\mu_t(x_t) \circ \mathrm{g}_t(w_t, z_t, m, d_t, \mathrm{y}_t(x_t)) = 0 \tag{10}$$

then the post-state actions are optimal *given the sequence of future discrete states.* (Note the partial derivatives are taken holding the time subscripted variables of the S-function fixed.)

For the following results, let $\{\mathrm{d}_t, \mathrm{y}_t\}_{t=0}^T$ be a sequence of feasible policy functions, and let $\vec{\boldsymbol{d}}_0$ and $\{m_t, y_t\}_{t=0}^T$ be generated by $\{\mathrm{d}_t, \mathrm{y}_t\}_{t=0}^T$.

Proposition 1. ***(Sufficient FOCs)*** *Assume there exists a sequence* $\{\mu_t\}_{t=0}^T$ *and* $\{\Lambda_t\}_{t=0}^T$ *of measurable functions such that* $\mu_t \colon X_t \to \mathbb{R}_+^{N_g}$ *and* $\Lambda_t \colon X_t \to \mathbb{R}_+^{N_M}$.

(1) If for every t *and* $x_t \in X_t$,

(i) m_t, $\mathrm{y}_t(x_t)$, $\mu_t(x_t)$ *and* $\Lambda_t(x_t)$ *are a saddle point of the S-function (*(7) - (10) *hold),*

(ii) $\mathbb{E}_{x_0}\left[\Lambda_{t+1}(x_{t+1})\mathrm{F}_t^m(d_t, y, w_{t+1})\right]^2 < \infty$, $\mathbb{E}_{x_0}\left[\Lambda_{t+1}\right]^2 < \infty$, $\mathbb{E}_{x_0}\left[\mu_t\right]^2 < \infty$, $\mathbb{E}_{x_0}\left[m_t\right]^2$ *and* $\mathbb{E}_{x_0}\left[y_t\right]^2 < 0$, *and*

(iii) $T < \infty$ *or* $\lim_{t\to\infty} \mathbb{E}_{x_0}\left[\Lambda_{t+1}(x_{t+1})\right] = 0$,

then $\{\mathrm{y}_t\}_{t=0}^T$ *solves* (**CS-DP**) *given* $\vec{\boldsymbol{d}}_0$.

(2) In addition, if $\mathrm{d}_t(x_t), \vec{\boldsymbol{d}}_{t+1}, \mathrm{y}_t(x_t) = \underset{d,\vec{\boldsymbol{d}}',y}{\arg\max}\, \mathrm{Q}_t^{\vec{\boldsymbol{d}}'}(x_t, d, y)$ *such that* $d, \vec{\boldsymbol{d}}', y$ *is feasible for each* t*, then* $\{\mathrm{d}_t, \mathrm{y}_t\}_{t=0}^T$ *solves* (**DP**).

Satisfying the FOCs (Item (1). of Proposition 1) is only a necessary condition for optimality in the sense of problem (**DP**). In the presence of non-convexity due to discrete choices, Item (2). of Proposition 1 must also hold. Item (2). says that each period, the entire future stochastic sequence of discrete choices implied by the post-state choice must be optimal. Note that, implicitly, the goal of upper envelope methods (Fella, 2014; Iskhakov et al., 2017; Druedahl and Jørgensen, 2017) is to remove post-state values that do not satisfy Item (2).

Below we verify that any solution will be a saddle point to the S-function, which is the main result of Section 3. To do so while circumventing the need to directly differentiate the value function, we prove the necessity of the Euler equation by applying variational arguments on the Hilbert space of random variables generated by feasible policies.[13]

Theorem 1. ***(Necessary FOCs)*** *If Assumption 1 and Assumptions D.1-D.3 hold, then there exists a measurable sequence* $\{\mu_t\}_{t=0}^T$ *and* $\{\Lambda_t\}_{t=0}^T$*,* $\mu_t \colon X_t \to \mathbb{R}_+^{N_g}$ *and* $\Lambda_t \colon X_t \to \mathbb{R}_+^{N_M}$*, such that for every* t*,* m_t*,* $\mathrm{y}_t(x_t)$*,* $\mu_t(x_t)$ *and* $\Lambda_t(x_t)$ *are a saddle point of the S-function (*(7) - (10) *hold).*

Corollary 1. *If the conditions of Proposition 1 hold, then* $\mathrm{v}_t^{\vec{\boldsymbol{d}}_t}(w_t, z_t, \tilde{m}_t) - \mathrm{v}_t^{\vec{\boldsymbol{d}}_t}(w_t, z_t, m_t) \leq \Lambda_t(x_t)(\tilde{m}_t - m_t)$ *for all* $m_t, \tilde{m}_t \in M_t$.

It follows that while the value function may not be differentiable at the kink points (recall Section 2.3.2), the shadow value $\Lambda_t(x_t)$ is a *'supgradient'* (i.e, $-\Lambda_t(x_t)$ is a subgradient of $-\mathrm{v}_t^{\vec{\boldsymbol{d}}_t}$) and defines a majorizing tangent plane to the value function conditional on a sequence of future discrete choices.

3.2. **The Euler equation in practice.** Let us return to examining the FOCs of the S-function and how they are used in computation. Expanding (7) and (8), we have

$$\begin{aligned}
\partial_m \mathbf{S}_t(m, y, \mu, \lambda \,|\, x_t, \boldsymbol{\Xi}_t) &= \partial_m \mathrm{u}_t(w_t, z_t, m, d_t, y) + \mu^\top \partial_m \mathrm{g}_t(w_t, m, z_t, d_t, y) - \lambda^\top = 0 \\
\partial_y \mathbf{S}_t(m, y, \mu, \lambda \,|\, x_t, \boldsymbol{\Xi}_t) &= \partial_y \mathrm{u}_t(w_t, z_t, m, d_t, y) \\
&\quad + \mu^\top \partial_y \mathrm{g}_t(w_t, z_t, m, d_t, y) + \mathbb{E}\Lambda_{t+1}(x_{t+1})^\top \partial_y \mathrm{F}_t^m(d_t, y, w_{t+1}) = 0
\end{aligned}$$

In the above FOCs, x_{t+1} is a function of y_t, x_t and the shock w_{t+1} that we held fixed while differentiating the S-function. By Proposition 1, sufficiency requires that given y_t, x_t and the expectation over the next period shock, a solution (m, y, μ, λ) to the above FOCs satisfies $y = \mathrm{y}_t(x_t)$, $m = m_t$ and (10). Equivalently, given a time t state variable x_t, Λ_{t+1} and fixed variables ξ_t,

[13]The method of proof recovers a real-valued recursive Euler equation (Shanker, 2017), where the recursive projection of history-contingent plans on an underlying Banach space generates recursive policy functions.

the FOCs imply that an optimal solution is a feasible root to the generalized Euler equation $y, \mu, \lambda \mapsto \mathbf{E}_t^{\xi_t}(y, \mu, \lambda \,|\, m_t)$, defined by the following components:

$$\mathbf{E}_{m,t}^{\xi_t}(y, \mu, \lambda \,|\, m_t) \colon = \partial_m \mathrm{u}_t(w_t, z_t, m_t, d_t, y) + \mu^\top \partial_{m_t} \mathrm{g}(w_t, z_t, m_t, y) - \lambda^\top \tag{11}$$

$$\begin{aligned}\mathbf{E}_{y,t}^{\xi_t}(y, \mu \,|\, m_t) \colon &= \partial_y \mathrm{u}_t(w_t, z_t, m_t, d_t, y) \\ &\quad + \mu^\top \partial_y \mathrm{g}(w_t, z_t, m_t, d_t, y) + \mathbb{E}_{x_t} \Lambda_{t+1}(x')^\top \partial_y \mathrm{F}_t^m(d_t, y, w_{t+1})\end{aligned} \tag{12}$$

$$\mathbf{E}_{\mu,t}^{\xi_t}(y, \mu \,|\, m_t) \colon = \mu \circ \mathrm{g}_t(w_t, z_t, m_t, d_t, y) \tag{13}$$

where $x' = \big(w_{t+1}, \mathrm{F}_t^d(d_t, w_{t+1}), \mathrm{F}_t^m(d_t, y, w_{t+1})\big)$, and such that $\mu > 0$. The Euler equation incorporates the intertemporal choice of the state (11), the intratemporal choice of the post-state (12), and the complementary slackness conditions associated with the constraints (13).

Following Iyengar and Kang (2005), we will refer to finding optimal values by finding roots to the Euler equation as the 'forward problem' – i.e., given Λ_{t+1}, one obtains optimal values of y_t, μ_t, λ_t for corresponding values of m_t and ξ_t to construct a policy function. Once the discrete choice function d_t has also been computed (see below), the time t policy functions can be recovered. Equation (11) then defines the iteration of the vector of shadow value functions as follows:

$$\Lambda_t(x_t) = \nabla_m \mathrm{u}_t(w_t, z_t, m_t, \mathrm{d}_t(x_t), \mathrm{y}_t(x_t)) + \nabla_m \mathrm{g}_t(w_t, m_t, \mathrm{d}_t(x_t), \mathrm{y}_t(x_t)) \mu_t(x_t), \tag{L}$$

and the time $t-1$ policy functions can then be recovered given Λ_t.

3.2.1. *Computation of the forward problem using FOCs on the active state space.* To detail the computation of the forward problem, without loss of generality, suppose there exists transformations of the functions u_t and g_t defined on an active state space $\bar{M}_t$. As such, let us define an 'active forward problem' that finds the roots of $(y, \mu, \lambda) \mapsto \bar{\mathbf{E}}_t(y, \mu, \lambda \,|\, \bar{m}_t)$, where

$$\bar{\mathbf{E}}_{\bar{m},t}(y, \mu, \lambda \,|\, \bar{m}_t) \colon = \partial_{\bar{m}} \bar{\mathrm{u}}_t(\bar{m}_t, y) + \mu_t^\top \partial_{m_t} \bar{\mathrm{g}}_t(\xi_t, \bar{m}_t, y) - \lambda^\top \tag{EO1}$$

$$\begin{aligned}\bar{\mathbf{E}}_{y,t}(y, \mu \,|\, \bar{m}_t) \colon &= \partial_y \bar{\mathrm{u}}_t(\bar{m}_t, y) \\ &\quad + \mu_t^\top \partial_y \bar{\mathrm{g}}(\xi_t, \bar{m}_t, y) + \mathbb{E} \Lambda_{t+1}(x')^\top \partial_y \mathrm{F}_t^m(d_t, y, w_{t+1})\end{aligned} \tag{EO2}$$

$$\bar{\mathbf{E}}_{\mu,t}(y, \mu \,|\, m_t) \colon = \mu \circ \bar{\mathrm{g}}_t(w_t, z_t, m_t, d_t, y) \tag{EO3}$$

The computational procedure using Euler equations proceeds as follows:

(A) Find the root of (**EO2**) given a continuous state $\bar{m}_t$ and fixed variables. Typically, one finds the roots of $(y, \mu) \mapsto \bar{\mathbf{E}}_{y,t}(y, \mu \,|\, \bar{m}_t)$ such that $\bar{\mathbf{E}}_{\mu,t}(y, \mu \,|\, m_t) = 0$ via numerical methods or EGM.[14]

(B) In the case of discrete-continuous problems, an upper-envelope method is used to select the optimal roots (i.e., the roots that satisfy Item (2). of Proposition 1). Once the optimal roots are found, the selection function ϕ_t can be used to construct the time t policy function

[14]Evaluating the roots of $y, \mu \mapsto \mathbf{E}_t^{\xi_t}(y, \mu \,|\, m_t)$ is equivalent to evaluating a policy under the Coleman-Reffett operator (Coleman, 1990; Reffett, 1996). See also Deaton (1991) and Li and Stachurski (2014) for more on policy iteration using the Euler equation.

$\mathrm{y}_{d_t,t}$. Equation (**EO1**) can then recover the shadow value $\lambda_{d_t,t}$ as a function of the time t state and fixed variables.

(C) The optimal *current period* discrete choices are computed by solving

$$d_t = \underset{d,\mathrm{y}_{d,t}(x_t)\in\Gamma_t(x_t)}{\arg\max} \mathrm{v}_t^d(x_t)$$

Once the current discrete choice function d_t has been computed, (**L**) can be used to recover λ_t.

To sum up, so far we (i) proved that the Euler equation is necessary to characterize optimality and also sufficient given a future sequence of discrete choices, and (ii) provided a straightforward way to derive the Euler equation in the presence of discrete choices and non-smooth constraints. With the Euler equations at hand, standard numerical root finding or EGM can then be used to implement the first step in the computational procedure just described above. However, the roots satisfying the FOCs are only sufficient to solve the dynamic programming problem given a future sequence of discrete choices. At any given time t, if the *entire future sequence of discrete choices* is not chosen to maximize the Q function *at each* t, then FOCs remain only necessary conditions. The following section turns to understanding when and how the inverse Euler equation is well-defined for step (A) above, and then turns to how to select the optimal roots in step (B).

4. Multidimensional inverse problem with discrete-continuous choices

This section formalizes the computation of policy functions via the inverse Euler equation in the general setup outlined above. Section 4.1 starts by defining an inverse optimization problem on the space of exogenous 'observed' variables, which we define as the product space of post-states and constraint multipliers. We then turn to the second key contribution of our paper – the necessary and sufficient conditions for this inverse problem to be well-defined. In cases where an inverse does not exist on the full-dimensional exogenous subspace of feasible observables, we also provide the conditions under which the exogenous grid can be defined as a subset of a lower-dimensional submanifold of the post-state space. We continue in Section 4.2 with the third key contribution of our paper – presenting the RFC algorithm that eliminates sub-optimal points in the presence of discrete choices. Importantly, we also provide error bounds for approximate solutions computed using the inverse Euler equation, which hold for the general case without discrete choices too.

Throughout this section we will fix time t, the shock realization w_t, the discrete state z_t, and the discrete choice d_t as a tuple ξ_t.

4.1. **Setup and invertibility.**

4.1.1. *Setup of inverse problem.* So far, EGM has been understood informally as a method to solve the policy function y_t by fixing y_t in an exogenous grid, and then finding values of the state m_t such that y_t satisfies the Euler equation. In contrast to the forward problem, this means EGM is an inverse optimization problem, where one solves for *inputs* m_t given *observed outputs* y_t. However, recalling the Euler equation (**EO2**), when constraints bind, the value of the multiplier μ_t will also determine the current state in an inverse problem. Our innovation is to formalize a general

inverse problem over the space of post-states and multipliers that contain the *observed information* we can use to determine the current state. In addition to the approach following naturally from recent advances in the theory of inverse problems (Iyengar and Kang, 2005), our method leads to a significant computational advantage since it sharply identifies which constraints bind from information in the exogenous grid.[15]

In terms of notation, we will use a_t, where $a_t = (y_{1,t}, \ldots, y_{N_Y,t}, \mu_{1,t} \ldots, \mu_{N_g,t})$, to denote an end-of-period 'observed' variable. Letting $\Upsilon_t \subset \mathbb{R}_+^{N_g}$ be the range of the function μ_t, we will use $A_t = Y_t \times \Upsilon_t$ to denote the space of end-of-period observed variables. Finally, define a function mapping the active state to observables $\sigma_t \colon \bar{M}_t \to A_t$ such that $\sigma_t(\bar{m}_t) = (\bar{y}_t(\bar{m}_t), \bar{\mu}_t(\bar{m}_t))$. The term $\sigma_t^{\vec{\boldsymbol{d}}_{t+1}}$ will refer to the function mapping the active state to the observed variables given feasible future discrete choices $[d_t, \vec{\boldsymbol{d}}_{t+1}]$.[16]

Not all possible observed variables will satisfy the constraints and complementary slackness condition (**EO3**). In particular, given ξ_t, let IB denote the set of all subsets of indices indexing the constraints on the active state space $\{\bar{\mathrm{g}}_{1,t} \ldots, \bar{\mathrm{g}}_{N_g,t}\}$. Fixing $\mathrm{IB}_l \in \mathrm{IB}$, let $\bar{\mathrm{g}}_t^l$ denote the vector of binding constraint functions. Solutions will belong to different 'constrained regions' $K_{l,t}$ associated with each subset $\mathrm{IB}_l \in \mathrm{IB}$ of binding constraints

$$K_{l,t} \colon = \left\{ (\bar{m}_t, y_t) \in \mathrm{Gr}\bar{\Gamma}_t, \mu_t \in \Upsilon_t \,\middle|\, \bar{\mathrm{g}}_t^l(\bar{m}_t, y_t) = 0,\ \mu_t \circ \bar{\mathrm{g}}_t(\bar{m}_t, y_t) = 0 \right\} \tag{14}$$

Recalling the definition of the projection π_A, the space $K_{l,t}^A \colon = \pi_A K_{l,t}$ denotes the possible observables within a constrained region that we could invert from, and $K_t^A = \bigcup_{l \in \mathrm{IB}} \pi_A K_{l,t}$ becomes the space of all observables satisfying the constraints and complementary slackness conditions (**EO3**).

Let us assume that the next period solution and the shadow value *function* Λ_{t+1} are known. Define the global EGM inverse problem[17] as

$$\begin{aligned}(\mathbf{IO}) \quad \Theta_t(y_t, \mu_t) \colon = \Big\{ \bar{m}_t \in \bar{M}_t \,\Big|\, \bar{\mathbf{E}}_{y,t}\left(y_t, \mu_t \,|\, \bar{m}_t\right) = 0, \\ \mathbf{d}_{t+1}(x_{t+1}) = \arg\max_{\vec{\boldsymbol{d}}'} \mathrm{Q}_t^{\vec{\boldsymbol{d}}'}(\bar{x}_t, y_t, d_t) \Big\}, \qquad (y_t, \mu_t) \in K_t^A\end{aligned}$$

where $x_{t+1} = (w_{t+1}, z_{t+1}, m_{t+1})$, $m_{t+1} = \mathrm{F}_t^m(d_t, y_t, w_{t+1})$, $\vec{\boldsymbol{d}}'$ is feasible,[18] and the function $\mathbf{d}_{t+1}$ maps the state variable x_{t+1} to future sequences of discrete choices. The definition incorporates Item (2). of Proposition 1 – i.e., finding a solution to the global inverse problem requires ensuring the future sequence of discrete choices implied by the post-state is optimal at time t. On the other hand, when we only compute roots to the Euler equation, we solve the following EGM inverse

[15]Druedahl and Jørgensen (2017) follows an approach where the inverse operator is defined over the product space of post-states and controls. In contrast, we define a formal inverse that maps directly to the FOCs of the S-function, and thus directly identifies where constraints bind. See Remark 2 below.

[16]Recall that d_t is fixed in this section.

[17]Without loss of generality, we have defined the EGM problem throughout this section on an active state space. When a strictly lower-dimensional active state space does not exist, the active state space can be trivially understood as the full current state space.

[18]Through a slight abuse of notation, we have defined the Q function on the active state space.

problem:

$$\textbf{(IO-FOC)}\quad \Theta_t^F(y_t,\mu_t)=\Big\{\bar{m}_t\in\bar{M}_t\,\big|\,\bar{\mathbf{E}}_{y,t}\left(y_t,\mu_t\,|\,\bar{m}_t\right)=0,\\ \mathbf{d}_{t+1}(x_{t+1})=\arg\max_{\boldsymbol{d}'}\mathrm{v}_{t+1}^{\boldsymbol{d}'}(x_{t+1},w_{t+1})\Big\},\qquad (y_t,\mu_t)\in K_t^A$$

Computing $\Theta_t^F(y_t,\mu_t)$ becomes the task of the initial root-finding step in EGM (Step (A) in the computational procedure above). As mentioned, a solution to the inverse problem $\Theta_t^F(y_t,\mu_t)$ that uses only the FOCs may not mean that the implied sequence of future discrete choices $\mathbf{d}_{t+1}(x_{t+1})$ is optimal. One has to remove sub-optimal roots from $\Theta_t^F(y_t,\mu_t)$ to arrive at (the possible empty set) $\Theta_t(y_t,\mu_t)$ using Step (B) above.[19] It follows that the inverse problem Θ_t may not be defined everywhere on a region K_t^A since for given y_t, Item (2). of Proposition 1 may not hold.

4.1.2. *Main results on invertibility.* Before we turn to selecting the optimal roots (whether analytically or numerically) in $\Theta_t^F(y_t,\mu_t)$, a natural question that arises is whether or not Θ_t^F is well-defined on neighbourhoods in K_t^A. Suppose we know that the Euler equation can be inverted at a point in K_t^A – i.e., we know that a solution exists for a future sequence of discrete choices. Does this mean we can construct an exogenous grid in a surrounding neighbourhood that is embedded in K_t^A? It may be that an inverse of the Euler equation is not defined on a full-dimensional neighbourhood of a solution point (see Section 5.2). And moreover, what is the dimension and structure of $\sigma_t^{\vec{\boldsymbol{d}}}(\bar{M}_t)$ compared to K_t?

The first assumption we require for invertibility is a standard rank condition on the constraints, which guarantees the multipliers are unique. The second assumption we require for invertibility is continuity of the policy function given a future sequence of discrete choices.[20]

Assumption (I.1) The cardinality of $\{i\,|\,\bar{\mathrm{g}}_{i,t}(\bar{m}_t,y_t)=0\}$ equals the rank of $\partial_y\bar{\mathrm{g}}_t(m_t,y_t)$ for every $(\bar{m}_t,y_t)\in\mathrm{Gr}\bar{\Gamma}_t$.

Assumption (I.2) For every feasible $\vec{\boldsymbol{d}}_{t+1}$, the optimal policy function $\bar{\mathrm{y}}_t^{\vec{\boldsymbol{d}}_{t+1}}$ is continuous.

We start with a necessary condition, and focus on the unconstrained case for simplicity. Suppose we could construct an exogenous grid in an open neighbourhood in Y_t and invert from it to a compact subset of the active state space. This situation can be dubbed 'pure EGM' since we invert from a full-dimensional subset of the exogenous space. The necessary condition tells us that for the inverse problem (**IO-FOC**) to be well-defined, the dimension of the post-state space must equal the dimension of the active state space. The necessary condition also applies to the general case where the policy function may not be globally invertible but may be locally invertible.[21] For this result, consider the restriction of $\bar{\mathrm{y}}_t$ to a compact non-trivial interval $\bar{C}\subset\bar{M}_t$, denoted by $\bar{\mathrm{y}}_t|_{\bar{C}}$.

[19]However, when the necessary FOCs are inverted, the implied sequence of future discrete choices $\vec{\boldsymbol{d}}_{t+1}$ still maximizes the next period value function.

[20]The continuity assumption is benign since given a future sequence of discrete choices, problem (**CS-DP**) can be solved as a standard concave dynamic programming problem, yielding continuous policies. Note that Feinberg et al. (2012) characterize existence and continuity even in the absence of bounded rewards or compact feasibility correspondences.

[21]For instance, potentially non-monotone, inverted U shaped policy functions.

Claim 1. *Let Assumption I.2 hold. If $\bar{\mathrm{y}}_t|_{\bar{C}}$ is injective, $\bar{\mathrm{y}}_t(\bar{C}) \subset \left\{y_t \,|\, \bar{\mathrm{g}}_t(\bar{m}, y_t) > 0, \bar{m} \in \bar{M}_t\right\}^{\mathrm{o}}$, and $\bar{\mathrm{y}}_t|_{\bar{C}}^{-1}$ is well-defined on an open neighbourhood in ${Y_t}^{\mathrm{o}}$, then $N_{\bar{M}} = N_Y$.*[22]

As for the sufficient conditions for invertibility of pure EGM, we can use Claim 1 to guide us: for pure EGM to be well-defined, the space we invert from must be a submanifold of the observables that is homeomorphic to $\mathbb{R}^{N_M}$. The inverse problem must then be defined on a manifold given by the graph of a continuous function of N_M 'exogenous observables' that determines the current state.

To formalize the sufficient condition, we use $\tilde{\mathrm{I}}_Y$ and $\tilde{\mathrm{I}}_\Upsilon$ to denote the $\tilde{N}_Y$, and $\tilde{N}_g$ indices of exogenous post-states and exogenous multipliers, respectively. Moreover, let $\tilde{Y}_t := \bigtimes_{i\in\tilde{\mathrm{I}}_Y} Y_{i,t}$, $\tilde{\Upsilon}_t := \bigtimes_{i\in\tilde{\mathrm{I}}_\mu} \Upsilon_{i,t}$ and $\tilde{A}_t = \tilde{Y}_t \times \tilde{\Upsilon}_t$. For a given a_t, note that we can fix the non-exogenous multipliers taking on values in $\Upsilon_t \setminus \tilde{\Upsilon}_t$ along $N_g - \tilde{N}_g$ indices, and the non-exogenous post-states taking on values in $Y_t \setminus \tilde{Y}_t$ along $N_Y - \tilde{N}_Y$ indices. We can then map the exogenous variables back to A_t using an embedding $\mathrm{em}_{\tilde{A}} \colon \tilde{A}_t \to A_t$. Next, we can also select elements from the vector $\bar{\mathbf{E}}_{a,t} := [\bar{\mathbf{E}}_{y,t}, \bar{\mathbf{E}}_{\mu,t}]$ along the N_Y indices of (i) multipliers associated with the binding constraints, and (ii) indices of post-states i such that $\partial_{y_i} \bar{\mathrm{g}}^l_t(\bar{m}_t, y_t) = 0$, to define a projection $\pi_{N_Y} \colon \mathbb{R}^{N_Y+N_g} \to \mathbb{R}^{N_Y}$.[23]

Theorem 2. ***(Invertibility of pure EGM)*** *Fix* $\mathrm{IB}_l \in \mathrm{IB}$. *If $\tilde{N}_Y + \tilde{N}_g = N_Y = N_M$ and there exists*

(1) $\bar{m}_t \in {M_t}^{\mathrm{o}}$ and $(y_t, \mu_t) \in \left(K^A_{l,t}\right)^{\mathrm{o}}$ such that $y_t = \bar{\mathrm{y}}^{\vec{\boldsymbol{d}}_{t+1}}_t(\bar{m}_t)$ for feasible $\vec{\boldsymbol{d}}_{t+1}$, and

(2) given (y_t, μ_t), an embedding $\mathrm{em}_{\tilde{A}} \colon \tilde{A}_t \to A_t$ and projection $\pi_{N_Y} \colon \mathbb{R}^{N_Y+N_g} \to \mathbb{R}^{N_Y}$ such that

$$\det \partial_{\bar{m}} \pi_{N_Y} \bar{\mathbf{E}}_{a,t} \left(\bar{m}, \mathrm{em}_{\tilde{A}}(\tilde{a})\right) \neq 0 \tag{15}$$

for all $(\bar{m}, \mathrm{em}_{\tilde{A}}(\tilde{a})) \in K_{l,t}$ with $\tilde{a} \in \left(\pi_{\tilde{A}} K_{l,t}\right)^{\mathrm{o}}$,

then there exists a continuous function φ and neighbourhood $U \subset \tilde{A}_t$ of $(\tilde{y}_t, \tilde{\mu}_t)$, such that for any $\tilde{e} \in U \subset \left(\pi_{\tilde{A}} K_{l,t}\right)^{\mathrm{o}}$, $\Theta^F_t\left(\varphi(\tilde{e})\right)$ is non-empty. Moreover, if $\bar{m} \in \Theta^F_t\left(\varphi(\tilde{e})\right)$, then $(\bar{m}, \varphi(\tilde{e})) \in K_{l,t}$.

Suppose we know a solution $(\bar{m}_t, y_t, \mu_t)$ exists in the interior of $K_{l,t}$. To check the conditions for Theorem 2, we must select $\tilde{N}_g$ exogenous multipliers and $\tilde{N}_Y$ exogenous post-states such that

(A) $\tilde{N}_g + \tilde{N}_Y = N_Y = N_{\bar{M}}$,

(B) the vector $\pi_{N_Y} \bar{\mathbf{E}}_{a,t} \left(\bar{m}, \mathrm{em}_{\tilde{A}}(\tilde{a})\right)$ contains indices of the gradient $\bar{\mathbf{E}}_{a,t} \left(\bar{m}, \mathrm{em}_{\tilde{A}}(\tilde{a})\right)$ associated with (i) the binding constraint multipliers IB_l, and (ii) the post-states i such that $\partial_{y_i} \bar{\mathrm{g}}^l_t(\bar{m}_t, y_t) = 0$,[24] and

[22] Through a slight abuse of notation, the superscript $\vec{\boldsymbol{d}}_{t+1}$ is dropped in Claim 1 to save on notation. One can view this result as the minimum requirement on dimensionality for pure EGM to be well-defined, even in the absence of discrete choices.

[23] Under Assumption I.1, the number of multipliers associated with the binding constraints is equal to the number of post-states such that $\partial_{y_i} \bar{\mathrm{g}}^{\mathrm{l}}_t(\bar{m}_t, y_t) \neq 0$. As such, the sum of post-states such that $\partial_{y_i} \bar{\mathrm{g}}^{\mathrm{b}}_t(\bar{m}_t, y_t) = 0$ and multipliers associated with the binding constraints is equal to N_Y.

[24] Note that $\tilde{a}_t = \pi_{\tilde{A}} a_t$ and for a_t, we have $a_t = \mathrm{em}_{\tilde{A}} \tilde{a}_t$, where $a_t = (y_t, \mu_t)$.

(C) the determinant of $\partial_{\bar{m}}\pi_{N_Y}\bar{\mathbf{E}}_{a,t}\left(\bar{m}, \mathrm{em}_{\tilde{A}}(\tilde{a})\right)$ is non-zero - i.e., (15) holds - for every $\tilde{a}$ in the interior of the constrained region along the exogenous variables, $\pi_{\tilde{A}}K_{l,t}$.

Under these conditions, we can construct an exogenous grid in an open neighbourhood of $\pi_{\tilde{A}}K_{l,t}$, and for $\tilde{a}$ in the grid, we are guaranteed to find $\bar{m}$ satisfying $\pi_{N_Y}\nabla_a\bar{\mathbf{S}}_t\left(\bar{m}, \mathrm{em}_{K^A}(\tilde{a}) \,|\, \bar{m}, \bar{\mathbf{\Xi}}_t\right) = 0$ (recall we have fixed Λ_{t+1}). To define the function φ in Theorem 2, for a permutation ν, the optimal policy given some $\vec{\boldsymbol{d}}_{t+1}$ and $\bar{m}$ will then be defined by $y = \left(y_{\nu_1}, \ldots, y_{\nu_{\tilde{N}_Y}}, y_{\nu_{\tilde{N}_Y+1},t}, \ldots, y_{\nu_{N_Y},t}\right)$, where $y = \pi_Y \mathrm{em}_{\tilde{A}}\tilde{a}$.[25] Under Assumption I.1, we can then recover the complete set of multipliers by solving for μ using $\mu \mapsto \nabla_a\bar{\mathbf{S}}_t\left(\bar{m}, y, \mu \,|\, \bar{m}, \bar{\mathbf{\Xi}}_t\right) = 0$.

Importantly, if we define the exogenous grid to be the subset of exogenous variables in $K^A_{l,t}$, since $K^A_{l,t}$ incorporates the complementary slackness conditions, we can recover *information about the optimally binding constraints* when we evaluate the inverse. The inverse solution will thus provide a state $\bar{m}$ such that the optimal solution given $\bar{m}$ and some $\boldsymbol{d}_{t+1}$ is in the region $K^A_{l,t}$. During computation, this avoids any costly secondary upper envelope loops to choose the optimal constraint.

Remark 2. *Fix* $\mathrm{IB}_l \in \mathrm{IB}$ *and consider the setting of Theorem 2. Suppose* $\tilde{a}_t$ *is a point in the exogenous grid, and we find* $\bar{m}_t$ *such that* $\bar{m}_t \in \Theta^F_t\left(\varphi(\tilde{a}_t)\right)$*. By Proposition 1, the observable* a_t*, with* $a_t = \varphi(\tilde{a}_t)$*, solves* (**CS-DP**) *given* $\bar{m}_t$*.*

So far, we assumed that within a constrained region $K_{l,t}$, a solution point exists and we studied the dimension and structure of an exogenous grid surrounding this point. A stronger result, guaranteeing that a solution exists everywhere in a constrained region, can then be obtained by checking the conditions of the well-known Poincaré-Miranda Theorem.

Corollary 2. *If* $a \in \pi_A K_{l,t}$ *and there exists* $I = \bigtimes_{i=1}^{N_M}[\hat{m}^{\min}_{i,t}, \hat{m}^{\max}_{i,t}] \subset \bar{M}_t$ *and* $(\iota_1, \ldots, \iota_{N_M}) \in \{-1, 1\}^{N_M}$ *such that for each* $j \in \{1, \ldots, N_M\}$ *and every* $\bar{m}_{k,t} \in [\hat{m}^{\min}_{k,t}, \hat{m}^{\max}_{k,t}]$ *with* $k \neq j$*, we have*

$$\iota_j\bar{\mathbf{E}}_{a,t}\left(\bar{m}_1, \ldots, \bar{m}_{j-1}, \ldots, \hat{m}^{\min}_j, \bar{m}_{j+1}, \ldots \bar{m}_{N_M}, \mathrm{em}_{\tilde{A}}(\tilde{a})\right) \leq \iota_j\bar{\mathbf{E}}_{a,t}\left(\bar{m}_1, \ldots, \bar{m}_{j-1}, \ldots, \hat{m}^{\max}_j, \bar{m}_{j+1}, \ldots \bar{m}_{N_M}, \mathrm{em}_{\tilde{A}}(\tilde{a})\right), \tag{16}$$

then $\Theta^F_t(a)$ *is well-defined.*

By examining (**EO2**) we see that verifying the conditions of the Poincaré-Miranda Theorem and (15) above is straightforward, as it only involves knowing how the primitive functions (i.e., the reward and constraint functions) behave as an argument of the state (see Section 5.1). The intuition for the proof (which we provide in the online appendix) of why this is true mirrors the deeper EGM intuition in Carroll (2006): the invertibility of the policy function and the convex constraint choice depends only on the mapping of information from the post-state to the state that, given the shadow value, is defined by the primitive functions.

[25] The variables $y_{\nu_1}, \ldots, y_{\nu_{\tilde{N}_Y}}$ in the vector y are the exogenous post-states, while the remaining variables are the post-states we held fixed to their value in y_t.

Let us now address the case where the dimension of the active state space is strictly lower than the post-state space. Pure EGM will not be well-defined. However, suppose the policy functions and multipliers are locally injective. So if we were to invert back from an exogenous grid, what would the structure of the exogenous grid be?

Assumption (I.3) For a compact set $\bar{C} \subset M_t$, and for each feasible $\vec{\boldsymbol{d}}_{t+1}$, the restriction of $\sigma_t^{\vec{\boldsymbol{d}}_{t+1}}$ to $\bar{C}$ is locally injective and continuous onto its own image.

Claim 2. *If Assumption I.3 holds, then for each feasible* $\vec{\boldsymbol{d}}_{t+1}$, $\dim(\sigma_t^{\vec{\boldsymbol{d}}_{t+1}}(\bar{C})) = N_{\bar{M}}$.

This claim answers our question by telling us that the dimension of the exogenous grid (which must be a subset of the image of the functions $\sigma_t^{\vec{\boldsymbol{d}}_{t+1}}$) must be the same as the dimension of the active state space, and even when none of the constraints bind, the image of the policy functions will be a lower-dimensional submanifold of the post-state space. Since $\sigma_t^{\vec{\boldsymbol{d}}_{t+1}}$ is an embedding, an implication is that a $N_{\bar{A}}$-dimensional submanifold of A_t can be constructed by a map from $\mathbb{R}^{N_{\bar{A}}}$ to $\mathbb{R}^{N_g+N_Y-N_{\bar{A}}}$ defined by the mapping of the post-state to the shadow value $y \mapsto \mathbb{E}_{x_t}\Lambda_{t+1}\partial_y \mathrm{F}_t^m(w_{t+1}, d_t, y)$ (see Section 5.2).

Corollary 3. *If Assumption I.3 holds, then* $\sigma_t(\bar{C})$ *is an* $N_{\bar{A}}$*-dimensional submanifold of* A_t*. Moreover, if* $N_{\bar{A}} < N_g + N_Y$*, then for each* $y, \mu \in \sigma_t(\bar{C})$*, there exists an open set* $O \subset \mathbb{R}^{N_{\bar{A}}}$*, an open set* $U \subset \mathbb{R}^{N_g+N_Y}$ *with* $y, \mu \in U$*, and a mapping* $\mathrm{sm}\colon \mathbb{R}^{N_{\bar{A}}} \to \mathbb{R}^{N_g+N_Y-N_{\bar{A}}}$ *such that*

$$Y_t \times \Upsilon_t \cap U = \Big\{ y, \mu \,\Big|\, \Big(y_{\iota_y(n_1+1)}, \ldots, y_{\iota_y(N_Y)}, \mu_{\iota_\mu(n_2+1)}, \ldots, \mu_{\iota_\mu(n_{N_g})}\Big) = \mathrm{sm}\left(y_{\iota_y(1)}, \ldots, y_{\iota_y(n_1)}, \mu_{\iota_\mu(1)}, \ldots, \mu_{\iota_\mu(n_2)}\right) \Big\}, \qquad n_1 + n_2 = N_{\bar{A}}$$

where ι_μ *and* ι_y *are permutations of the indices of the multipliers and post-states, respectively.*

4.1.3. *Computation of the inverse problem.* To approximate optimal policy functions, we define the computational procedure as tuple

$$\left(\Theta_t^F, (K_{l,t})_{l\in \mathrm{IB}}, (\mathcal{A}_{l,t})_{l\in \mathrm{IB}}, \kappa_t\right)$$

The inverse problem Θ_t^F and constrained regions K_t are defined above. The set of grid points $\mathcal{A}_{l,t}$ denotes the exogenous grid, which must satisfy

$$\mathcal{A}_{l,t} \subset \bigcup_{\vec{\boldsymbol{d}}_{t+1}} \sigma_t^{\vec{\boldsymbol{d}}_{t+1}}(\bar{M}_t) \bigcap K_{l,t} \tag{17}$$

where the union is taken over all future discrete choices such that $[d_t, \vec{\boldsymbol{d}}_{t+1}]$ is feasible given some $\bar{m}_t \in \bar{M}_t$. The term $\sigma_t^{\vec{\boldsymbol{d}}_{t+1}}(\bar{M}_t)$ is the image of the active state space under the observable function. For each l, we can set up $\mathcal{A}_{l,t}$ to be a finite subset of an $N_{\bar{M}}$-dimensional space of exogenous variables in the image of the policy functions within the constrained region $K_{l,t}$. In practice, note that the points $\mathcal{A}_{l,t}$ can be setup as a space of variables (such as control variables) isomorphic ('equivalent') to the observables (see application 5.1 below). The function κ_t is a 'grid pasting function' where

$\kappa_t \colon \bigcup_{\vec{\boldsymbol{d}}_{t+1}} \sigma_t^{\vec{\boldsymbol{d}}_{t+1}}(\bar{M}_t) \to \mathbb{R}^{N_{\bar{M}}}$. This function allows us to join the different constrained regions into a single $N_{\bar{M}}$-dimensional space. Placing restrictions on the curvature of κ_t will be key in implementing the RFC algorithm and its asymptotic error bound, as we discuss below.

Elements of $\mathcal{A}_{l,t}$ will be denoted $a_{t,i}^{\#}$ and depending on the context, we use $a_{t,i}^{\#}$ and $(y_{t,i}^{\#}, \mu_{t,i}^{\#})$ interchangeably. The computation of the inverse problem fixes - or 'observes' - a finite sequence (i.e., exogenous grid), and the objective is to obtain the corresponding endogenous grid $\mathcal{M}_t^{\star} \subset M_t$ by solving the inverse problem (**IO**) such that

$$m_{t,i}^{\#} \in \Theta_t(y_{t,i}^{\#}, \mu_{t,i}^{\#}), \qquad \forall y_{t,i}^{\#}, \mu_{t,i}^{\#} \in \mathcal{A}_t, m_{t,i}^{\#} \in \mathcal{M}_t \tag{18}$$

Next, let $x_{t,i}^{\#} = (w_t, m_{t,i}^{\#}, z_t)$ and let $I^{\mathcal{A}}$ be the index set for the exogenous grid. Further grids are set as below:

(1) The grid of 'objective values' $\mathcal{V}_t^{\star} = \left\{ \mathrm{Q}_t(x_{t,i}^{\#}, d_{t,i}, y_{t,i}^{\#}) \right\}_{i \in I^{\mathcal{A}}}$ obtained by evaluating (**Q**).

(2) The subset of the exogenous grid points that are optimal given their associated endogenous grid point $\mathcal{A}_t^{\star} \colon = \left\{ y_{t,i}^{\#}, \mu_{t,i}^{\#} \in \mathcal{A}_t \middle| \, \Theta_t(y_t^{\#}, \mu_{t,i}^{\#}) \neq \varnothing \right\}$.

The endogenous grid generated by the necessary conditions (**IO-FOC**) will be denoted by $\mathcal{M}_t^{\mathrm{F}}$, with $\mathcal{M}_t^{\mathrm{F}} \subset \bar{M}_t$, satisfying

$$m_{t,i}^{\#} \in \Theta_t^{\mathrm{F}}(y_{t,i}^{\#}, \mu_{t,i}^{\#}), \qquad \forall y_{t,i}^{\#}, \mu_{t,i}^{\#} \in \mathcal{A}_t, m_{t,i}^{\#} \in \mathcal{M}_t^{\mathrm{F}}$$

As such, define

(3) The grid of objective values of the future choice-specific value functions $\mathcal{V}_t^{\mathrm{F}} = \left\{ \mathrm{Q}_t(x_{t,i}^{\#}, d_t, y_{t,i}^{\#}) \right\}_{i \in I^{\mathcal{A}}}$ obtained by evaluating (**Q**).[26]

(4) The grid of supgradients of the future discrete choice-specific value functions $\mathcal{V}_t^{\mathrm{F}}$ with respect to the state as $\nabla \mathcal{V}_t^{\mathrm{F}}$ (recall Corollary 1 and evaluate the supgradients using (**L**) at the exogenous and endogenous grid points).

Remark 3. *It follows from Item (1). of Proposition 1 that any $v_{t,i}^{\#} \in \mathcal{V}_t^F$ will correspond to a future sequence of discrete choices $\mathbf{d}_{t+1}(x'_{t+1,i})$ that are optimal at time $t+1$. In particular, $v_{t,i}^{\#} = \mathrm{u}_t(x_{t,i}^{\#}, d_t, y_{t,i}^{\#}) + \mathbb{E}_{x_t^{\#}} \mathrm{v}_{t+1}^{\vec{\boldsymbol{d}}_{t+1}}(x'_{t+1,i}) = \mathrm{v}_t^{\vec{\boldsymbol{d}}_t}(x_{t,i}^{\#})$, where $\vec{\boldsymbol{d}}_t = [d_t, \mathbf{d}_{t+1}(y_{t+1,i}^{\#})]$, $x_{t,i}^{\#} = (w_t, z_t, m_{t,i}^{\#})$ and $x'_{t+1,i} = \mathrm{F}_t(d_t, y_{t,i}^{\#}, w_{t+1})$.*

Remark 4. *Since the FOCs are necessary, $\mathcal{M}_t^{\star} \subset \mathcal{M}_t^F$, where the inclusion may be strict.*

4.2. **Rooftop-cut algorithm.** When $\mathcal{M}_t^{\star} \subset \mathcal{M}_t^{\mathrm{F}}$ is a proper subset, the task is to remove sub-optimal points in the endogenous grid $\mathcal{M}_t^{\mathrm{F}}$, and produce a set as close as possible to $\mathcal{M}_t^{\star}$. To do so, we propose the RFC algorithm.

[26] Recall from Section 2.3.1 that objective values may be sub-optimal at time t.

Recall from our discussion below (**BE-2**) and Remark 3 that each exogenous grid point $a^{\#}_{t,i}$ implies a particular future stochastic sequence of discrete choices $\boldsymbol{d}_{t+1}$. We do not know, however, if this future sequence is optimal given the current state implied by the endogenous grid point $m^{\#}_{t,i}$. The RFC algorithm uses the *supgradients of the future choice-specific value functions* (recall Figure 1) in the $\nabla\mathcal{V}^{\mathrm{F}}_t$ grid to determine if neighbouring points in the endogenous grid are optimal or sub-optimal. To implement the algorithm in practice, we first set a 'jump detection threshold' $\bar{J} > 0$ and a 'search radius' $\rho_r > 0$. Let I^{F} denote the index set of the points in $\mathcal{M}^{\mathrm{F}}_t$, and initialize $I^{\mathrm{cut}} \equiv \{\}$. The RFC algorithm proceeds as follows:

Box 1: RFC algorithm

For each $j \in I^{\mathrm{F}}$,

(1) Construct a tangent plane to the future choice-specific value function at $m^{\#}_{t,j}$ using the supgradient $\nabla v^{\#}_{t,j} \in \nabla\mathcal{V}^{\mathrm{F}}_t$ at the value $v^{\#}_{t,j} \in \mathcal{V}^{\mathrm{F}}_t$. The tangent plane is given by $m^{\#} \mapsto \nabla v^{\#}_{t,j} \circ (m^{\#} - m^{\#}_{t,j})$.

(2) For each l such that $m^{\#}_{t,l} \in \mathbb{B}_{\rho_r}(m^{\#}_{t,j}) \cap \mathcal{M}^{\mathrm{F}}_t$,

(i) if the tangent plane $m^{\#} \mapsto \nabla v^{\#}_{t,j}(m^{\#} - m^{\#}_{t,j})$ dominates the value $v^{\#}_{t,l}$ at the endogenous grid point $m^{\#}_{t,l}$ – i.e., $\nabla v^{\#}_{t,j} \circ (m^{\#}_{t,l} - m^{\#}_{t,j}) > v^{\#}_{t,l}$, and

(ii) if the relative difference between the exogenous grid points at j and l in the distance κ_t is greater than $\bar{J}$ – i.e., $\frac{\kappa_t(a^{\#}_{t,j} - a^{\#}_{t,l})}{\|m^{\#}_{t,l} - m^{\#}_{t,j}\|} > \bar{J}$,

then append l to I^{cut}.

Once the steps above are completed for each $j \in I^{\mathrm{F}}$, the optimal grid points are recovered by deleting the dominated neighbouring points from the endogenous grid, thus constructing an index set $I^{\mathrm{RFC}} := I \setminus I^{\mathrm{cut}}$. The grids constructed by the RFC algorithm will be

$$\mathcal{M}^{\mathrm{RFC}}_t = \left\{m^{\#}_{t,i}\right\}_{i \in I^{\mathrm{RFC}}}, \mathcal{A}^{\mathrm{RFC}}_t = \left\{a^{\#}_{t,i}\right\}_{i \in I^{\mathrm{RFC}}}, \mathcal{V}^{\mathrm{RFC}}_t = \left\{v^{\#}_{t,i}\right\}_{i \in I^{\mathrm{RFC}}} \tag{19}$$

To intuitively understand the algorithm, consider Figure 2 that demonstrates the RFC algorithm for a stylized one-dimensional problem. To simplify exposition, assume κ_t is the identity function and assume we are considering an unconstrained problem. Both plots show the endogenous grid points in $\mathcal{M}^{\mathrm{F}}_t$ on the x-axis. On the y-axis, the left plot shows the points of the future choice-specific values in $\mathcal{V}^{\mathrm{F}}_t$, while the right plot shows the policy function values in the grid $\mathcal{Y}^{\mathrm{F}}_t$. The points $(m^{\#}_{t,i-1}, v^{\#}_{t,i-1})$, $(m^{\#}_{t,i}, v^{\#}_{t,i})$, $(m^{\#}_{t,i+2}, v^{\#}_{t,i+2})$, and $(m^{\#}_{t,i+3}, v^{\#}_{t,i+3})$ are on the upper envelope, while the points $(m^{\#}_{t,i-1}, a^{\#}_{t,i-1})$, $(m^{\#}_{t,i}, a^{\#}_{t,i})$, $(m^{\#}_{t,i+2}, a^{\#}_{t,i+2})$, and $(m^{\#}_{t,i+3}, a^{\#}_{t,i+3})$ define the optimal policy. In contrast, the point $(m^{\#}_{t,i+1}, v^{\#}_{t,i+1})$ is not on the upper envelope, and the policy $(m^{\#}_{t,i+1}, a^{\#}_{t,i+1})$ is not optimal. Here note that the point $(m^{\#}_{t,i+1}, a^{\#}_{t,i+1})$ 'jumps' from the point $(m^{\#}_{t,i}, a^{\#}_{t,i})$ (see the right plot) since it is associated with a different future sequence of discrete choices. The point $(m^{\#}_{t,i+1}, a^{\#}_{t,i+1})$ it is also dominated by the tangent to the future choice-specific value function at $(m^{\#}_{t,i}, v^{\#}_{t,i})$ (see the left plot), and is thus removed. In contrast, while the point $(m^{\#}_{t,i+3}, a^{\#}_{t,i+3})$ also 'jumps' from the point $(m^{\#}_{t,i}, a^{\#}_{t,i})$, this point dominates the tangent, and is thus retained. The point $(m^{\#}_{t,i+4}, a^{\#}_{t,i+4})$ is similarly removed.

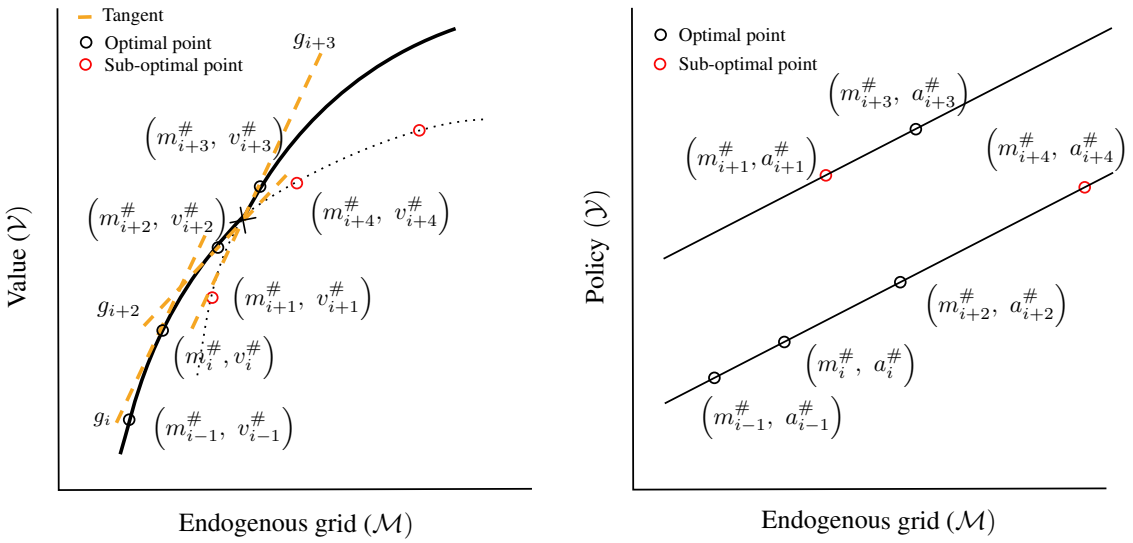

Figure 2. The RFC algorithm

How do we choose the pasting function κ_t, the jump detection threshold $\bar{J}$, and the search radius ρ_r? We briefly describe the practical considerations here and turn to a formal analysis in the next section. For each feasible future sequence of discrete choices $\boldsymbol{d}_{t+1}$, we require κ_t to be a function such that the function $\acute{\kappa}_t^{\boldsymbol{d}_{t+1}}$ defined by $\bar{m} \mapsto \kappa_t(\sigma_t^{\boldsymbol{d}_{t+1}}(\bar{m}) \,|\, \Lambda_{t+1}^{\boldsymbol{d}_{t+1}})$ is Lipshitz with constant no greater than L_1, and has a Lipshitz inverse with constant no greater than L_2. This allows us to relate the exogenous grid spacing to the endogenous grid spacing. In many applications, the function mapping the exogenous variables to appropriately chosen 'controls' or post-states (e.g., consumption) can serve as the evaluation of κ_t.[27]

The choice of the jump detection threshold can be made based on the maximum possible curvature of the functions $\acute{\kappa}^{\boldsymbol{d}_{t+1}}$ given a future sequence of discrete choices $\boldsymbol{d}_{t+1}$. For instance, in a standard income fluctuation problem, the marginal propensities to consume are bounded above by one and below by a constant that can be derived analytically (Carroll, 2023), allowing us to set $\bar{J} \geq 1$. The search radius, on the other hand, can be chosen to be greater than the maximum 'spacing between neighbouring points' in the endogenous grid. Consider constructing an exogenous grid such that for a particular grid size $|\mathcal{A}_t|$ there exists ϵ with $\|\kappa^{\boldsymbol{d}_{t+1}}(a_{t,i}^{\#}) - \kappa^{\boldsymbol{d}_{t+1}}(a_{t,j}^{\#})\| < \epsilon$ for neighbouring exogenous points; then the search radius can be set to $\rho_r = 2\epsilon L_2$ since the maximum possible distance between the associated endogenous grid points will be ϵL_2.

Finally, depending on the particular application, it may be more practicable to apply RFC iteratively or sequentially via search or scan methods to reduce the need to compute all pairwise tangent conditions. We discuss these practical implications in Section 5.

[27]To fix the intuition regarding the grid pasting function, consider the simple case of a standard income fluctuation problem (Li and Stachurski, 2014) with no discrete choices, liquid asset y_t, an artificial liquidity constraint $y_t \geq 0$, and i.i.d earnings shocks. We can set $\kappa_t(\mu, y) = \partial \mathrm{u}^{-1}(\mu + \mathbb{E}_{x_t}\Lambda_{t+1}(\mathrm{F}_t^m(w_{t+1}, y)))$, where $\partial \mathrm{u}^{-1}$ is the inverse of the marginal utility and μ is the multiplier associated with the liquidity constraint. For the unconstrained region, $\kappa_t(0, y_t) = \partial \mathrm{u}^{-1}(\mathbb{E}_{x_t}\Lambda_{t+1}(y_t))$. Controlling the distance between the consumption implied by the exogenous grid allows us to control the distance between points in the endogenous grid, across both constrained and unconstrained regions.

4.2.1. *Intersection points.* We can use the first order information in the RFC algorithm to easily add an approximation of the intersection points of two different future choice-specific value functions. In Figure 2, the point $\times$ is an approximation of the intersection of the future choice-specific value functions. When a neighbouring point l lies above a tangent plane to the future choice-specific value function at j, the intersection point can be found by finding the intersection of the two lines $p \mapsto (m^{\#}_{t,j}, v^{\#}_{t,j}) + p \circ \nabla v^{\#}_{t,j}(m^{\#}_{t,l} - m^{\#}_{t,j})$ and $p \mapsto (m^{\#}_{t,l}, v^{\#}_{t,l}) + p \circ \nabla v^{\#}_{t,l}(m^{\#}_{t,j} - m^{\#}_{t,l})$.

We can also add the optimal policy at the intersection points. In particular, suppose $m^{\#}_{t,\times}$ is an approximated intersection point between $m^{\#}_{t,l}$ and $m^{\#}_{t,j}$. We can perform a nearest neighbour search around the point $m^{\#}_{t,j}$ in the original grid $\mathcal{A}_t$ and find neighbouring points $\left\{m^{\#}_{t,i}, y^{\#}_{t,i}\right\}_i$ such that the observable values do not 'jump' from the point j. An interpolant can be constructed using these neighbouring points to locally approximate the optimal policy given the optimal future discrete choice implied by $m^{\#}_{t,j}$. This interpolant can be evaluated at $m^{\#}_{t,\times}$ to produce an approximate policy $y^{\#}_{t,\times}$. To ensure jumps in the policy are approximated, an approximate policy interpolated using neighbours to the policy at $m^{\#}_{t,l}$ can also be attached at an arbitrarily small distance from $m^{\#}_{t,\times}$. We note that in applications with many states, it may be more practicable to approximate policies at the intersection by nearest neighbour interpolation, a procedure that performs well in the application 5.1.2).

4.2.2. *Vectorization.* A key advantage of the RFC algorithm is that it can be made highly efficient using vectorized computation (Harris et al., 2020), making it possible for multidimensional discrete-continuous applications to exploit the massive parallelism offered by GPUs. In particular, the deviation in the objective values between a point and its other neighbouring points can be represented by $(\mathcal{V}_t - \mathcal{V}^{\text{neigh}}_t)$, where $\mathcal{V}^{\text{neigh}}_t$ is a matrix such that each j'th row is a list of the objective values of the ι-neighbouring points to j. Similarly, $|(\mathcal{Y}_t - \mathcal{Y}^{\text{neigh}}_t)/(\mathcal{M}_t - \mathcal{M}^{\text{neigh}}_t)|$ becomes a matrix of gradients of each policy value to neighbouring policy values. We can then compute the sub-optimal points via the Boolean operation

$$I^{\text{cut}} = \Big((\mathcal{M}_t - \mathcal{M}^{\text{neigh}_t}) \otimes \nabla\mathcal{V}_t > (\mathcal{V}_t - \mathcal{V}^{\text{neigh}_t})\Big) \circ \Big(|\mathcal{Y}_t - \mathcal{Y}^{\text{neigh}_t}|/\|(\mathcal{M}_t - \mathcal{M}^{\text{neigh}_t}\| > \bar{J}\Big), \tag{20}$$

where $\otimes$ is the tensor dot product defined over the appropriate axes. The result I^{cut} is a tensor whose i, j'th entry determines whether grid point j is sub-optimal. Since this equation represents the RFC algorithm using tensor algebra, the algorithm can be easily programmed without 'loops' to exploit array programming packages such as NumPy, Google JAX and CUDA (Sargent and Stachurski, 2024).

4.2.3. *Convergence and error bound.* In this subsection, Theorem 2 or Claim 2 conditions will be in force. We now state the assumptions used for our theoretical results on the RFC algorithm.

The first assumption states that we formally study the exogenous grid as a simplicial complex generated by the image of the grid pasting functions.

Assumption (E.1) For each feasible $\vec{\boldsymbol{d}}_{t+1}$, the points $\kappa_t(\sigma_t^{\vec{\boldsymbol{d}}_{t+1}}(\bar{M}_t) \bigcap \mathcal{A}_t)$ are asymptotically dense in $\kappa_t(\sigma_t^{\vec{\boldsymbol{d}}_{t+1}}(\bar{M}_t))$ and generate a simplicial complex $\mathbb{K}^{\vec{\boldsymbol{d}}_{t+1}}$.

The second assumption requires that we can control the grid spacing of the exogenous grid using the pasting function. Let $|\mathcal{A}_t|$ denote the number of exogenous grid points, and let $\epsilon_{|\mathcal{A}_t|}$ denote the maximum circumcircle of the simplicies in $\cup_{\vec{\boldsymbol{d}}_{t+1}} \mathbb{K}^{\vec{\boldsymbol{d}}_{t+1}}$.

Assumption (E.2) $\lim_{|\mathcal{A}_t| \to \infty} \epsilon_{|\mathcal{A}_t|} = 0.$

The third assumption requires that the policy functions translated by the pasting function (*conditional on a future sequence of discrete choices*) are monotone and do not 'change' arbitrarily fast. The assumption works to bound the distance between endogenous grid points, and is rather standard in economic applications since quantities like marginal propensities to save and consume are bounded (White, 2015; Carroll, 2023) – recall the definition of $\acute{\kappa}^{\boldsymbol{d}_{t+1}}$ above.

Assumption (E.3) The family of functions $\left\{\acute{\kappa}^{\boldsymbol{d}_{t+1}}\right\}_{\boldsymbol{d}_{t+1}}$ are monotone and bi-Lipshitz with Lipshitz constant of $\acute{\kappa}^{\boldsymbol{d}_{t+1}}$ no greater than L_1, and Lipshitz constant of $\acute{\kappa}^{\boldsymbol{d}_{t+1},-1}$ no greater than L_2.[28]

For a function f, let us define $\mathrm{f} \circ \sigma_t^{\mathrm{INT}}$ to be the linear interpolant of the function $\mathrm{f} \circ \sigma_t$ constructed using Barycentric coordinates of simplicies in the Delaunay triangulation of $\mathcal{M}_t^{\mathrm{RFC}}$ and the points $\mathrm{f}(\mathcal{A}^{\mathrm{RFC}})$.

Theorem 3. ***(Asymptotic error bound)*** *Let Assumptions E.1 - E.3 hold and assume $L_2\epsilon < \rho_r$. If for each feasible $\boldsymbol{d}_{t+1}$, $\mathrm{f} \circ \sigma_t^{\boldsymbol{d}_{t+1}}$ is Lipshitz with constant no greater than L_0, then for any $\bar{m}_t \in \bar{M}_t$ such that $\sigma_t(\bar{m}_t) \in K_{t,l}^{\mathrm{o}}$, there exists $\epsilon_{|\mathcal{A}_t|}$ such that for all $\epsilon < \bar{\epsilon}$, $\|\mathrm{f} \circ \sigma^{\mathrm{INT}}(\bar{m}_t) - \mathrm{f} \circ \sigma(\bar{m}_t)\| < \epsilon(1 + 2L_0L_2)$.*

While this is a worse case pointwise result, we do not require assumptions on the number or type of jump discontinuities or monotonicity of the policy function. Furthermore, in applications, we are typically interested in the asymptotic accuracy of the moment conditions generated by integrating the policy function. The above result implies that if the functions $\mathrm{f} \circ \sigma_t$ are bounded, then moment conditions will converge as the exogenous grid size increases.

Corollary 4. *Let Assumption 1 hold. If $\left[\mathrm{f} \circ \sigma(\bar{m}_t^{\vec{\boldsymbol{d}}_{t+1}})\right]^p$ is uniformly bounded and measurable for all feasible $\vec{\boldsymbol{d}}_{t+1}$, then for $p \geq 1$, $\mathbb{E}\left[\mathrm{f} \circ \sigma^{\mathrm{INT}}(\bar{m}_t)\right]^p \to \mathbb{E}\left[\mathrm{f} \circ \sigma(\bar{m}_t)\right]^p$ as $|\mathcal{A}_t| \to \infty$.*

The uniform boundedness condition is straightforward to satisfy if, for instance, the policy functions are bounded. Note that including the points of intersection between future choice-specific value functions does not affect the error bounds, since the intersection points are also a first order approximation. Moreover, the methods that include the intersection points - such as those proposed by Iskhakov et al. (2017) - will at best be subject to the error bound above since they rely on constructing secants between overlapping future choice-specific value functions.

[28]The family of $\boldsymbol{d}_{t+1}$ are all future discrete choices such that $[d_t, \mathbf{d}_{t+1}]$ is feasible given some $\bar{m}_t \in \bar{M}_t$.

5. Applications

This section illustrates our theoretical results on the Euler equation inverse and the RFC algorithm using two well-known dynamic optimization applications on (i) savings and retirement choice with unemployment risk a' la Druedahl and Jørgensen (2017), and (ii) housing investments with adjustment frictions similar to those in Kaplan and Violante (2014); Yogo (2016); Dobrescu et al. (2022). The online appendix and the public software repository additionally include two other RFC applications to further illustrate the generality of our approach – i.e., the one-dimensional savings and labor force participation choice model in Iskhakov et al. (2017), and the consumption-saving model with housing adjustment costs in Fella (2014).

5.1. **Application 1: Savings and retirement choice.**

Our first application is the model in Druedahl and Jørgensen (2017) to which we subsequently add an extra constraint to (i) demonstrate the RFC performance, and also (ii) show how using Theorem 2 to determine where constraints bind *on the exogenous grid* can significantly improve computational speed and deal with the added complexity. In this context, let T be finite and consider the problem of an agent who chooses a post-state $y_t = (y_{f,t}, y_{p,t})$ that consists of end-of-period financial assets $y_{f,t}$ and pension assets $y_{p,t}$ to maximize lifetime utility. The continuous state variables of the problem are start-of-period financial assets $m_{f,t}$ and pension assets $m_{p,t}$. Thus, the continuous state space is $M_t = M_{f,t} \times M_{p,t} = \mathbb{R}^2_+$ and the post-state space is $Y_t = Y_{f,t} \times Y_{p,t} = \mathbb{R}^2_+$. Each period, the agent can choose whether or not to work next period, with $d_t = 1$ denoting employment and $d_t = 0$ retirement. The discrete state variable z_t captures the agent's employment status at the beginning of the period. Accordingly, the discrete choice space and discrete state space are $D_t = \{0, 1\}$ and $Z_t = \{0, 1\}$, respectively.

Turning to the transition functions, we note that financial assets evolve according to

$$m_{f,t+1} = (1 + r_f) y_{f,t} + z_{t+1} w_{t+1} + (1 - z_{t+1}) (\bar{w} + (1 + r_p) y_{p,t}) \tag{21}$$

where $\bar{w}$ is the unemployment benefit paid to retirees. The rate of return on financial assets is r_f, and the rate of return on pension assets is r_p. If an agent is employed at the beginning of a period, they receive stochastic earnings w_t, with w_t being log-normally distributed. If, however, the agent retires, they receive their pension balance as a lump-sum payment. The transition function for pension assets is then given by

$$m_{p,t+1} = z_{t+1}(1 + r_p) y_{p,t} \tag{22}$$

where pension assets only accumulate for workers. Each period the agent works ($z_t = 1$), they can make pension contributions $c_{p,t}$ that translate to end-of-period pension assets as

$$y_{p,t} = m_{p,t} + \chi(c_{p,t}) \tag{23}$$

where χ is a function representing the incentives to make pension contributions, with $\chi(x) = 1 + \bar{\chi} \log(1 + x)$, $\bar{\chi} > 0$. Finally, employment status evolves according to $z_{t+1} = d_t z_t$ and so, a retired agent cannot work again.

The feasibility correspondence for the problem Γ_t, is given by (i) the borrowing constraint on total assets $y_t \geq 0$, (ii) the liquidity constraint preventing pension withdrawals before retirement

$$\chi^{-1}(y_{p,t} - m_{p,t}) \geq 0, \tag{24}$$

(iii) the constraint preventing retirees from making further pension contributions when retired

$$y_{p,t}(1 - z_t) = 0, \tag{25}$$

and (iv) a constraint that caps pension contributions to be no greater than earnings

$$c_{p,t} \leq w_t \tag{26}$$

In what follows we will use constraint (iv) to demonstrate the utility of Theorem 2. While new compared to Druedahl and Jørgensen (2017), note that this constraint captures a key feature of many pension plans such as the 401(k) in the U.S. and superannuation plans in Australia.

Turning to payoffs, the agent enjoys consumption according to a CRRA utility function with parameter $\rho > 1$, and discounts time according to a factor $\beta \in (0, 1)$. An agent who decides to remain employed pays a utility cost $\delta > 0$. Thus, the Bellman equation for a worker who chooses to continue working becomes[29]

$$\mathrm{v}_t^1(w_t, 1, m_{f,t}, m_{p,t}) = \max_{y_t \in \Gamma_t(x_t)} \left\{ \frac{c_t^{\rho-1}}{\rho - 1} + \beta \mathbb{E}_{x_t} \left[\mathrm{v}_{t+1}(w_{t+1}, 1, m_{f,t+1}, m_{p,t+1}) \right] \right\} - \delta \tag{27}$$

where $c_t = m_{f,t} - y_{f,t} - c_{p,t}$. In contrast, the Bellman equation for a worker who chooses to retire next period becomes

$$\mathrm{v}_t^0(w_t, 1, m_{f,t}, m_{p,t}) = \max_{y_t \in \Gamma_t(x_t)} \left\{ \frac{c_t^{\rho-1}}{\rho - 1} + \beta \mathbb{E}_{x_t} \left[\mathrm{v}_{t+1}(0, m_{f,t+1}) \right] \right\} \tag{28}$$

where $c_t = m_{f,t} - y_{f,t} - c_{p,t}$. (To emphasise the distinction between those who continue working and those who choose to retire, we have written each individual state variable as an argument for the value function through the slight abuse of the notation we have established.) The optimal discrete choice each period is $d_t = \arg\max_{d \in \{0,1\}} \mathrm{v}_t^d(w_t, 1, m_{f,t}, m_{p,t})$. The decision problem for the retiree is standard and we omit it for brevity - see (Druedahl and Jørgensen, 2017) for details.

5.1.1. *Necessary Euler equation.* The utility function in this application will be unbounded below since the state space of the financial assets is $\mathbb{R}_+$. If the agent arrives into a period with state $m_{f,t} > 0$, then for $\Gamma_t(x_t)$ to be compact-valued, $\Gamma_t(x_t)$ must include the feasible choice of zero consumption where utility hits $-\infty$. On the other hand, if we exclude zero consumption from the feasible choices given x_t, then $\Gamma_t(x_t)$ will not be compact-valued. Thus, even without the issue of non-differentiability due to discrete choices, the generalized results by Rincón-Zapatero and Santos (2009) cannot be directly applied to derive the Euler equation. Moreover, the solution will not always be an interior point in $\Gamma_t(x_t) \cap \Gamma_t^{-1}(y_{t+1})$ since a worker may not make pension contributions in one or more consecutive periods. Thus, the Clausen and Strub (2020) results cannot be applied

[29]Recall our discussion of current period discrete choice-specific value functions in Section 2.3.1.

either, as the pension withdrawal constraint (25) may bind in consecutive periods.[30] However, it is straightforward to verify that Assumptions D.1 - D.3 hold (see online appendix). In terms of the general setup of Section 2.2, note that $\mathrm{u}_t(w_t, z_t, m_t, d_t, y_t) = \beta^t \frac{c_t^{\rho-1}}{\rho-1} =: \beta^t \varphi_u(c_t)$. We can now use the S-function to derive the necessary Euler equations. In particular, at time t, the FOCs of the S-function are[31]

$$\varphi_u'(c_t) = \mu_{f,t} + \beta \mathbb{E}_{x_t}\left[\mathrm{u}_{t+1}'(c_{t+1})\,(1+r_f)\right] = \mu_{f,t} + \beta \mathbb{E}_{x_t}\lambda_{t+1,f}\,(1+r_f) \tag{29}$$

$$\varphi_u'(c_t) = \mu_{p,t} - \mu_{\bar{p},t} + \mathbb{E}_{x_t}\lambda_{p,t+1}\,(1+r_p)\left(1+\chi'(c_{p,t})\right) \tag{30}$$

$$\mu_{f,t} y_{f,t} = 0 \tag{31}$$

$$\mu_{p,t} c_{p,t} = 0 \tag{32}$$

$$\mu_{\bar{p},t}\,(c_{p,t} - w_t) = 0 \tag{33}$$

$$\lambda_{p,t} = z_t \mathbb{E}_{x_t}\lambda_{p,t+1}\,(1+r_p) + (1-z_t)\varphi_u'(c_t) \tag{34}$$

$$\lambda_{f,t} = \varphi_u'(c_t) \tag{35}$$

where we have $c_t = m_{f,t} - y_{f,t} - c_{p,t}$, $c_{p,t} = y_{p,t} - m_{p,t} - \chi(c_{p,t})$. The multiplier $\mu_{f,t}$ is associated with the liquidity constraint on financial assets, the multiplier $\mu_{p,t}$ is associated with the pension withdrawal constraint (24), and $\mu_{\bar{p},t}$ is associated with the pension contributions cap constraint (26). For a worker, there are six combinations of binding constraints defined by $y_t \geq 0$, (24) and (26). We index the binding constraints by $\mathrm{IB} = \left\{\mathrm{ucon}, \mathrm{dcon}, \mathrm{acon}, \mathrm{con}, \overline{\mathrm{dcon}}, \overline{\mathrm{con}}\right\}$. Following the steps (A) - (C) below Theorem 2, we can construct each region, its corresponding exogenous variables, associated grids, and the projected Euler equation as follows:

- ucon: No constraints bind – $K^A_{\mathrm{ucon},t} = \{a_t \,|\, y_{f,t} \geq 0, y_{p,t} \geq 0, \mu_t = 0\}$, $\mathcal{A}_{\mathrm{ucon},t} \subset \{y_t \,|\, y_t \geq 0\}$. The exogenous variables are $y_{f,t}$ and $y_{p,t}$, and $\pi_{N_Y}\mathbf{E}_{a,t}$ is given by (29) and (30).
- dcon: Lower pension constraint binds (24) binds – $K^A_{\mathrm{dcon},t} = \{a_t \,|\, y_t \geq 0, \mu_{f,t} = 0, \mu_{p,t} \geq 0, \mu_{\bar{p},t} = 0\}$, $\mathcal{A}_{\mathrm{dcon},t} \subset \{y_t | y_t \geq 0\}$. The exogenous variables are $y_{f,t}$ and $y_{p,t}$, and $\pi_{N_Y}\mathbf{E}_{a,t}$ is given by (29) and (32).
- acon: Financial assets constraint binds ($y_{f,t} \geq 0$) – $K^A_{\mathrm{acon},t} = \{a_t \,|\, y_{f,t} = 0, y_{p,t} \geq 0, \mu_{f,t} \geq 0, \mu_{p,t}, \mu_{\bar{p},t} = 0\}$, $\mathcal{A}_{\mathrm{acon},t} \subset \{y_{p,t}, c_t \,|\, y_{p,t} \geq 0, c_t \geq 0\}$. The exogenous variables are $\mu_{f,t}$ and $y_{p,t}$, and $\pi_{N_Y}\mathbf{E}_{a,t}$ is given by (30) and (31).
- con: All lower constraints bind – $K^A_{\mathrm{con},t} = \{a_t | y_{f,t} = 0, y_{p,t} \geq 0, \mu_{f,t} \geq 0, \mu_{p,t} \geq 0, \mu_{\bar{p},t} = 0\}$, $\mathcal{A}_{\mathrm{con},t} \subset \{y_{p,t}, c_t \,|\, y_{p,t} \geq 0, c_t \geq 0\}$. The exogenous variables are $y_{p,t}$ and $\mu_{f,t}$, and $\pi_{N_Y}\mathbf{E}_{a,t}$ is given by (31) and (32).
- $\overline{\mathrm{dcon}}$: Pension cap constraint 26 binds – $K^A_{\overline{\mathrm{dcon}},t} = \{a_t \,|\, y_t \geq 0, \mu_{f,t} = 0, \mu_{p,t} = 0, \mu_{\bar{p},t} \geq 0\}$, $\mathcal{A}_{\overline{\mathrm{dcon}},t} \subset \{y_t \,|\, y_t \geq 0\}$. The exogenous variables are $y_{f,t}$ and $y_{p,t}$, and $\pi_{N_Y}\mathbf{E}_{a,t}$ is given by (29) and (33).

[30] If we additionally impose the risk of zero earnings, application-specific approaches such as Li and Stachurski (2014) and Ma et al. (2022) also fail since there will be no strictly positive upper bound on the marginal utility of consumption (Carroll, 2023).

[31] We write the shadow values and multipliers in their current value form below.

- $\overline{\text{con}}$: Financial assets and pension cap constraints ($y_{f,t} \geq 0$ and 26)bind – $K^{A}_{\overline{\text{con}},t} = \{a_t \,|\, y_{f,t} = 0, y_{p,t} \geq 0, \mu_{f,t} \geq 0, \mu_{p,t} = 0, \mu_{\bar{p},t} \geq 0\}$, $\mathcal{A}_{\overline{\text{con}},t} \subset \{y_{p,t}, c_t \,|\, y_t \geq 0\}$. The exogenous variables are $y_{p,t}$ and $\mu_{f,t}$, and $\pi_{N_Y}\mathbf{E}_{a,t}$ is given by (29) and (33).

Recall that exogenous grids $\mathcal{A}_{l,t}$ are constructed as points equivalent to the exogenous variables.[32] The first four constrained regions are common with Druedahl and Jørgensen (2017), while $\overline{\text{dcon}}$ and $\overline{\text{con}}$ arise due to the pension cap constraint. Additionally, note that to formally define the regions as above, we required the multipliers to obey the complementary slackness conditions. In general, additional constraints can lead to an exponential increase in the number of regions. The core idea of Theorem 2 is that by evaluating the inverse operator Θ^F_t at exogenous grid points in each region, we are able to obtain prior information on the optimal constraint choice that binds from the exogenous grid. This means we do not need to interpolate separate policy functions for each constrained region across all possible exogenous grid points. A number of grid points are thus eliminated since they are not solutions to Θ^F_t, and the remaining points across the regions can be combined into a single irregular grid over which we need to apply an upper envelope method, and interpolate only once regardless of the number of constraints. (In the online appendix we verify that by Theorem 2 and Proposition 2, we can construct an exogenous grid $\mathcal{A}_t$ around a solution point in the two-dimensional regions above.)

Finally, we can choose end-of-period pension assets and consumption evaluated at the exogenous grid, denoted by $a \mapsto (\hat{y}_{p,t}(a), \hat{c}_t(a))$, as the grid pasting function κ_t. The functions $\kappa_t^{\vec{\boldsymbol{d}}_{t+1}}$ are then the pension policy function and the consumption function $(\mathrm{y}_{p,t}^{\vec{\boldsymbol{d}}_{t+1}}, \mathrm{c}_t^{\vec{\boldsymbol{d}}_{t+1}})$. Since the marginal propensity to consume (MPC) of $\mathrm{c}_t^{\vec{\boldsymbol{d}}_{t+1}}$ will be bounded above by 1 and the slope of $\mathrm{y}_{p,t}^{\vec{\boldsymbol{d}}_{t+1}}$ bounded above by 2, we can set $\bar{J} > 2$. Moreover, letting M_t be compact, the inverse of $(\mathrm{y}_{p,t}^{\vec{\boldsymbol{d}}_{t+1}}, \mathrm{c}_t^{\vec{\boldsymbol{d}}_{t+1}})$ will also be Lipshitz and L_2 will be bounded above by $\frac{1}{\underline{\text{MPC}}}$, where $\underline{\text{MPC}}$ is the lower bound on the MPC (Carroll, 2023). As such, we can pick $\rho_r > \frac{2\epsilon}{\underline{\text{MPC}}}$ as the search radius, where ϵ is the distance between exogenous grid points in the '$(y_{p,t}, c_t)$-space'.

5.1.2. *Numerical implementation.* To illustrate the RFC algorithm for the retirement choice model above, we use the baseline calibration in Druedahl and Jørgensen (2017), both with and without a pension cap. To benchmark our method, we implement the solution algorithm using (i) the nested EGM suggested by Druedahl (2021) (NEGM), (ii) EGM using our RFC algorithm and a Delaunay triangulation (RFC w. Delaunay),[33] and (iii) EGM using the upper envelope method in Druedahl and Jørgensen (2017) (G2EGM). To implement RFC efficiently, we apply the vectorized algorithm iteratively to nearest neighbours of a subset of total points in the endogenous grid until no new sub-optimal points are found.

[32]Formally, for instance, $\mathcal{A}_{\text{acon},t} \subset \{y_{p,t}, c_t \,|\, y_{p,t} \geq 0, c_t \geq 0\} \cong \{y_{p,t}, \mu_{f,t} \,|\, y_{p,t} \geq 0, \mu_{f,t} \geq 0\}$.

[33]In implementing the EGM step for RFC, we use the Euler equations defined above to identify the binding constraints on the exogenous grid. Because of the RFC speed, note we can use a standard SciPy implementation of Delaunay triangulation in Python to optimally interpolate the policy function. Delaunay triangulations are the optimal triangulation that minimize the linear interpolation error on an irregular grid (Chen and Xu, 2004). While Druedahl and Jørgensen (2017) and Ludwig and Schön (2018) point out that Delaunay may come at significant computational cost, this example shows that using the appropriate software libraries can make Delaunay triangulations highly efficient without sacrificing the EGM speed advantage.

Figure 3 shows the constrained segments in a model without a pension cap, from the set IB within both the endogenous and exogenous grid at time $t = T - 13$. Each region of the exogenous grid in the right plot is a two-dimensional submanifold of the space of observable variables, defined by the sets $K_{l,t}$.[34] The sub-optimal red points noted in the figure are points within the regions that are removed by the RFC algorithm. Our contribution in Theorem 2 showed that inverting from these regions leads to the optimal solution. The power of Theorem 2 is thus demonstrated here by the isomorphic mapping of each segment from the right plot to the corresponding region in the endogenous grid in the left plot. Note that while different constrained regions overlap in the exogenous grid, they form disjoint segments in the endogenous grid – i.e., each point in the endogenous grid is associated with a unique optimal solution and a unique optimal constraint choice. With two additional constrained regions, since the regions are disjoint in the endogenous grid, the number of endogenous grid points that the RFC with the interpolation step has to process remains similar.

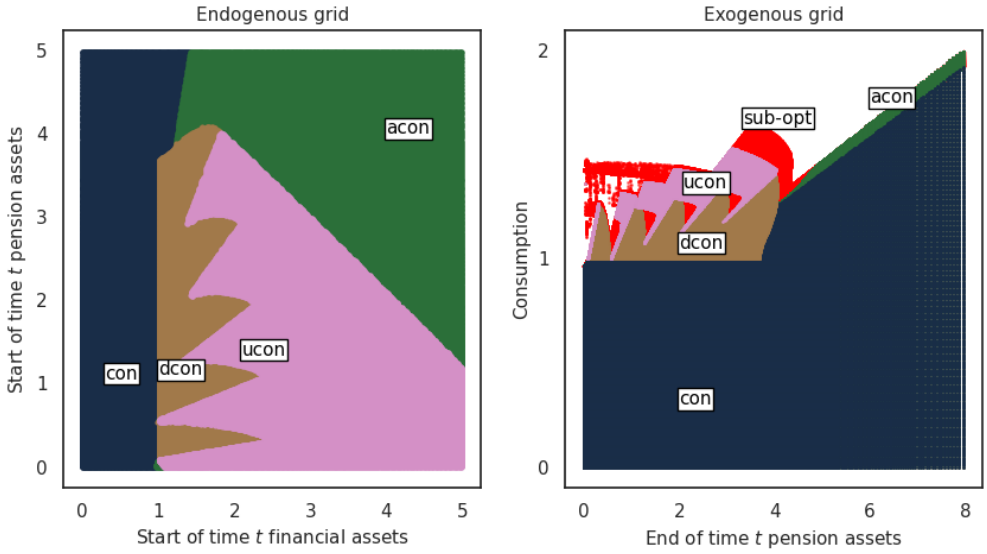

Figure 3. Constrained regions with no cap on pensions

In terms of accuracy, we find that our RFC implementation is comparable to the upper envelope method in terms of relative Euler error, and even dominates slightly on the mean Euler error (see online appendix). Turning to speed, the left plot of Figure 4 shows the time it takes to solve the model without a pension cap for 15 periods. We see that our implementation (i.e., RFC with interpolation via Delaunay triangulation) and the upper envelope method (G2EGM) are comparable in terms of total time efficiency, and both are about twice as fast as NEGM. Note here, however, also that the time actually taken by the RFC alone is about 25% of the total time. This gain in speed, due to the vectorized RFC and calculating the optimal constraints from the exogenous grid, also allows us to use an off-the-shelf SciPy implementation of Delaunay triangulation to interpolate

[34]This manifold is isomorphic to the regions in Figure 3 defined over consumption and end-of-period pension assets.

over the endogenous grid, thereby significantly simplifying the EGM implementation for the model.

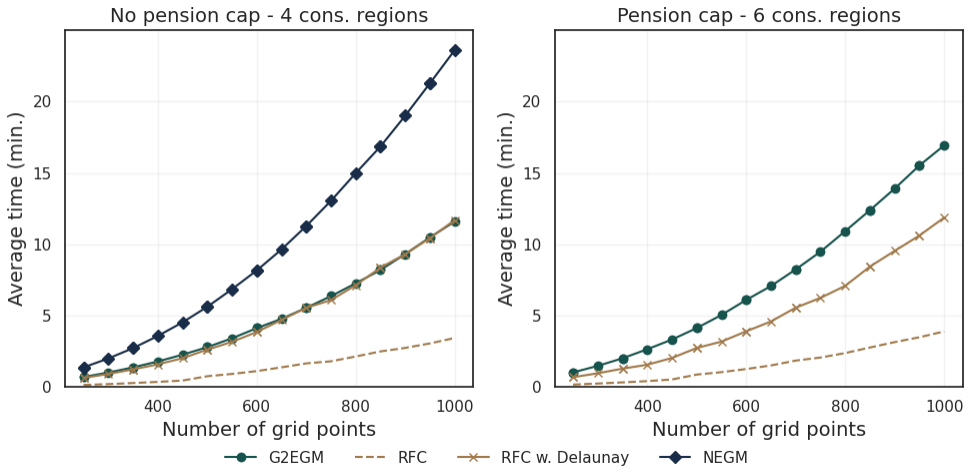

Figure 4. Computational speed benchmarking

Finally, the right plot of Figure 4 shows how our implementation handles two additional constrained regions. The time taken to invert the Euler equation and run RFC in this case remains almost identical to the one without the additional regions, since we already have the optimal points that are not constrained from the exogenous grid. So we only need to perform the upper envelope step using RFC and interpolate once over a similar number of grid points as when we had only four constrained regions. If we did not use Theorem 2, however, and evaluated the upper envelope of each region's policy function separately as in Druedahl and Jørgensen (2017), we would have a 50% increase in total computational time due to the 50% increase in the number of constrained regions.

5.2. **Application 2: Housing investments with adjustment frictions.** We now turn to demonstrating our results in the stylized version of a veritable workhorse in the housing frictions literature (Kaplan and Violante, 2014; Yogo, 2016; Dobrescu et al., 2022). To do so while maintaining comparability, our model specification closely follows Druedahl (2021). Interestingly, while the example in this section also features two dimensions of savings – one for liquid (financial) assets and one for illiquid (housing) assets – pure EGM cannot be applied. Rather, optimal financial and housing assets occupy a one-dimensional submanifold of the post-state space. In this case, we show that EGM can still be employed to gain significant speed and numerical accuracy, using a root-finding step to construct an exogenous grid.

5.2.1. *Model environment.* Let T be finite. Consider an agent who chooses a post-state $y_t = (y_{f,t}, y_{h,t})$ consisting of end-of-period financial assets $y_{f,t}$ and housing assets $y_{h,t}$. The continuous state variables for the problem are start-of-period financial assets $m_{f,t}$ and housing assets $m_{h,t}$. Thus, the post-state space is $Y_t = Y_{f,t} \times Y_{h,t} = \mathbb{R}^2_+$, and the continuous state space is $M_t = M_{f,t} \times M_{h,t} = \mathbb{R}^2_+$. The agent also makes a discrete choice d_t, where investing in and out of housing

stock can only be made if $d_t = 1$. Otherwise, if $d_t = 0$ then $y_{h,t+1} = m_{h,t+1}$, and we must have

$$(y_{h,t} - m_{h,t})(1 - d_t) = 0 \tag{36}$$

Investments can be made in and out of the stock of $m_{f,t}$ without friction. Turning to the transition functions, note that financial assets evolve according to

$$m_{f,t+1} = (1 + r)y_{f,t} + w_{t+1} \tag{37}$$

where financial assets earn a rate of return r, and w_{t+1} denotes stochastic earnings. We assume that housing brings no returns so

$$m_{h,t+1} = y_{h,t+1} \tag{38}$$

and that the equations describing the non-negativity constraint on total resources $y_t \geq 0$ and the friction on housing $(y_{h,t} - m_{h,t})(1 - d_t) = 0$ define the value of the feasibility correspondence $\Gamma_t(x_t)$.

Turning to per-period rewards, the agent enjoys utility from non-housing consumption c_t and from the end-of-period housing stock $y_{h,t}$. We assume per-period rewards given by[35]

$$\mathrm{u}_t(m_t, y_t) = \beta^t \underbrace{\left[\frac{c_t^{\rho-1} - 1}{\rho - 1} + (1 - \alpha) \ln(y_{h,t}) \right]}_{:=\varphi^u(c_t, y_{h,t})} \tag{39}$$

where consumption satisfies

$$c_t = m_{f,t} + d_t m_{h,t} - y_{a,t+1} - d_t(1 + \tau)y_{h,t+1} \tag{40}$$

Adjusting the housing stock to a value $y_{h,t}$ requires a payment of $\tau y_{h,t}$ with $\tau > 0$, leading to a non-concave continuation value. Turning to the agent's recursive problem, the Bellman equation for an agent who decides not to adjust their housing stock becomes

$$\mathrm{v}_{0,t}(w_t, m_t) = \max_{y_t \in \Gamma_t(x_t)} \{\varphi_t^u(c_t, y_{h,t}) + \beta \mathbb{E}_{x_t} \mathrm{v}_{t+1}(w_{t+1}, m_{a,t+1}, m_{h,t})\} \tag{41}$$

where $c_t = m_{f,t} - y_{f,t}$. (To emphasize the distinction between adjusters and non-adjusters, we have written each state variable as an argument for the value function through the slight abuse of the notation we have established.) The Bellman equation for an agent adjusting their housing stock is

$$\mathrm{v}_{1,t}(w_t, m_{f,t}, m_{h,t}) = \max_{y_t \in \Gamma_t(x_t)} \{\varphi_t^u(c_t, y_{h,t}) + \beta \mathbb{E}_{x_t} \mathrm{v}_{t+1}(w_{t+1}, m_{a,t+1}, m_{h,t+1})\} \tag{42}$$

where $c_t = m_{f,t} + m_{h,t} - y_{f,t} - (1 + \tau)y_{h,t+1}$. For both Bellman equations, (37), (38) and (40) must hold. The optimal discrete choice each period is $d_t = \arg \max_{d \in \{0,1\}} \mathrm{v}_t^d(w_t, m_{f,t}, m_{h,t})$ and

$$\mathrm{v}_t(w_t, m_{f,t}, m_{h,t}) = \max_{d \in \{0,1\}} \mathrm{v}_t^d(w_t, m_{f,t}, m_{h,t}) \tag{43}$$

[35]To ease exposition, in what follows we assume that utility from housing and non-housing consumption is separable. A constant elasticity of substitution (CES) specification of consumption and housing is computationally straightforward to implement, and an example is provided in our online repository.

5.2.2. *Necessary Euler equations.* For periods prior to the terminal one, the recursive Euler equation (**EO2**) for financial assets is

$$\partial_c \varphi^u(c_t, y_{h,t}) = \mu_{a,t} + \beta \mathbb{E}_{x_t} \Lambda_{a,t+1}(w_{t+1}, m_{f,t+1}, m_{h,t+1}) \geq \beta(1+r)\mathbb{E}_{x_t} \partial_c \varphi^u(c_{t+1} y_{h,t+1}), \tag{44}$$

where c_t and c_{t+1} obeys (40), and the state transition equations (37) and (38) hold. Note also that in the last term in (44), the optimal $t+1$ policy function is $y_{t+1} = \mathrm{y}_{t+1}(w_{t+1}, m_{f,t+1}, m_{h,t+1})$. If $d_t = 1$, the recursive Euler equation for housing stock is

$$\begin{aligned}(1+\tau)\partial_c \varphi^u(c_t, y_{h,t}) = \mu_{h,t} + \mathbb{E}_{x_t} \Lambda_{h,t+1}(w_{t+1}, m_{f,t+1}, m_{h,t+1}) + \partial_h \varphi^u(c_t, y_{h,t}) \\ \geq \underbrace{\mathbb{E}_{x_t} \sum_{k=t}^{\iota-1} \beta^{t-\iota} \partial_{y_h} \varphi^u(c_k, y_{h,k+1})}_{\substack{\text{Marginal value of} \\ \text{housing services}}} + \underbrace{\mathbb{E}_{x_t} \beta^{t-\iota} \left(\partial_c \varphi^u(c_\iota, y_{h,\iota+1})\right)}_{\substack{\text{Marginal value of} \\ \text{liquidating housing at time } \iota}}.\end{aligned} \tag{45}$$

The intuition of the financial assets Euler equation (44) is standard. The housing Euler equation (45), however, features a stochastic time subscript ι defined as the next period when $d_\iota = 1$. Since the next time the stock is adjusted will be stochastic, ι becomes a random stopping time. Equation (45) then tells us that the shadow value of the housing stock is the discounted expected value of the stock *when the stock is next liquidated*, along with the stream of housing services provided up to the time of liquidation. (See Section 4.1 in Kaplan and Violante (2014) for a similar intuition.)

Once we find the time t solution (by following the steps below), let $\mathrm{y}_{f,d,t}$ and $\mathrm{y}_{h,d,t}$ denote the optimal choice-specific policy functions conditional on the time t discrete choice, with $d \in \{0,1\}$. Given the optimal policy functions, the iteration of the shadow values is

$$\Lambda_{h,t}(x_t) = \mathrm{d}_t(x_t)\partial_c \varphi^u(c_t, y_{h,t}) + \beta \mathbb{E}_{x_t}(1 - \mathrm{d}_t(x_t)) \left[\mathbb{E}_{x_t} \Lambda_{h,t+1}(x_{t+1}) + \partial_{y_h} \varphi^u(c_t, y_{h,t})\right], \text{and} \tag{46}$$

$$\Lambda_{a,t}(x_t) = \partial_{y_h} \varphi^u(c_t, y_{h,t}) \tag{47}$$

where $x_t = (w_t, m_{f,t}, m_{h,t})$, $c_t = m_{f,t} + \mathrm{d}_t(x_t) m_{h,t} - \mathrm{d}_t(x_t)\mathrm{y}_{a,\mathrm{d}_t(x_t),t}(x_t) - \mathrm{y}_{h,\mathrm{d}_t(x_t),t}(x_t)(1+\tau)$ and $y_{h,t} = \mathrm{y}_{h,\mathrm{d}_t(x_t),t}(x_t)$.

Remark 5. *If $d_{t+1} = 0$, then $d_{t+1}, y_{t+1} \in \Gamma_{t+1}(x_{t+1})$ if and only if $y_{h,t+1} = m_{h,t+1}$, and thus $y_{h,t}$ cannot be in the interior of the set $\{y \,|\, d_{t+1}, y_{t+1} \in \Gamma_{t+1}(\mathrm{F}_t^m(d_t, y, w_{t+1}))\}$. Thus, Theorem 6 by Clausen and Strub (2020) cannot be applied since the interiority assumption on next period policy in the one-shot deviation problem is violated.*

5.2.3. *Computation using EGM and the RFC algorithm.* Suppose we know v_{t+1} and $\Lambda_{h,t+1}$. We can first apply standard EGM with RFC to evaluate $y_{f,0,t}$ for *non-adjusters*, since only one Euler equation - i.e., equation (44) - will hold. For each possible time t housing state $m_{h,t}$ in the housing grid $\mathcal{Y}_{h,t}$ and exogenous state w_t, we can approximate $\mathrm{y}_{f,0,t}(w_t, \cdot, m_{h,t})$ by first setting an exogenous grid (over the constrained and unconstrained regions) of $y_{f,t}$ and c_t values (holding $y_{h,t} = m_{h,t}$ fixed as no adjustment occurs), and then creating an endogenous grid of time t financial assets $m_{f,t}$ using

(44) and the budget constraint (40). The RFC algorithm can then be applied to eliminate sub-optimal points, allowing us to obtain an approximation of the policy function $\mathrm{y}_{f,0,t}$.

For *adjusters*, Bellman equation (42) shows that their solution only depends on total resources $\bar{m}_t = m_{f,t} + m_{h,t}$. Thus, the dimension of the active state space $\mathbb{R}_+$ (i.e., one) is less than the dimensions of the post-states (i.e., two). By Proposition 3, there will then be a one-dimensional submanifold embedded in the post-state space from which the adjuster Euler equations can be inverted (see online appendix for details). The submanifold will thus be characterized by financial and housing asset values that satisfy the Euler equation 45. To construct the exogenous grid, note we can evaluate time t consumption c_t, given the values of $y_{h,t}$ and $y_{f,t}$, as

$$c_t = \partial_c \varphi^{u,-1}((1+r)\beta \Lambda_{f,t+1}(m_{f,t+1}, m_{h,t+1}), y_{h,t}) \tag{48}$$

where $\partial_c \varphi^{u,-1}$ is the analytical inverse of $\partial_c \varphi^u$ in its first argument. The procedure to evaluate the policy functions for adjusters is then as follows:

Box 2: RFC and EGM for the adjuster policy function

(1) Fix ξ_t and a uniform grid over values of the exogenous variable $y_{h,t}$, $\mathcal{Y}_{h,t}$. Initialise the exogenous grid as an empty array ($\mathcal{A}_t$), current period objective values ($\mathcal{V}_t$), and an endogenous wealth grid ($\mathcal{M}_t$).

(2) For each $y^{\#}_{h,t,i} \in \mathcal{Y}_{h,t}$:

  (i) Evaluate the P multiple roots to (45) in terms of $y_{f,t}$, with c_t evaluated by (48), and $y_{h,t}$ fixed as $y^{\#}_{h,t,i}$. Collect the roots in a tuple $(y^{\#}_{f,t,i_0}, \ldots, y^{\#}_{f,t,i_j}, y^{\#}_{f,t,i_P})$. Append $((y^{\#}_{f,t,i_0}, y^{\#}_{h,t,i}), \ldots, (y^{\#}_{f,t,i_P}, y^{\#}_{h,t,i}))$ to $\mathcal{A}_t$.

  (ii) For each root in $(y^{\#}_{f,t,0}, \ldots, y^{\#}_{f,t,i_j}, \ldots, y^{\#}_{f,t,i_P})$, evaluate the endogenous grid points of total resources $(\bar{m}^{\#}_{t,0}, \ldots, \bar{m}^{\#}_{t,j}, \ldots, \bar{m}^{\#}_{t,P})$ using the budget constraint

$$\bar{m}^{\#}_{t,i_j} = y^{\#}_{f,t,i_j} + (1+\tau) y^{\#}_{h,t,i} + c_t$$

  and evaluate the current period objective values $(v^{\#}_{t,0}, \ldots, v^{\#}_{t,i_j}, \ldots, v^{\#}_{t,i_P})$ as

$$v^{\#}_{t,i_j} = u(c_t, y^{\#}_{h,t,i}) + \beta \mathbb{E}_{w_t} \mathrm{v}_{t+1}(w_{t+1}, (1+r) y^{\#}_{f,t,i_j}, y^{\#}_{h,t,i})$$

  (iii) Append the P endogenous grid points to $(\bar{m}^{\#}_{t,0}, \ldots, \bar{m}^{\#}_{t,j}, \ldots, \bar{m}^{\#}_{t,P})$ to $\mathcal{M}_t$, and $(v^{\#}_{t,0}, \ldots, v^{\#}_{t,i_j}, \ldots, v^{\#}_{t,i_P})$ to $\mathcal{V}_t$.

(3) Apply the RFC algorithm to $\mathcal{V}_t$, $\mathcal{A}_t$, and $\mathcal{M}_t$ and recover $\mathcal{M}^{\mathrm{RFC}}_t$, $\mathcal{V}^{\mathrm{RFC}}_t$, and $\mathcal{Y}^{\mathrm{RFC}}_t$.

We apply these steps for each w_t in the exogenous shock grid; with $\mathrm{y}_{h,1,t}$ and $\mathrm{y}_{f,1,t}$ approximated on a uniform grid, we can then construct $\mathrm{y}_{h,t}$ and $\mathrm{y}_{f,t}$ in the standard way by solving (43).

Finally, note that the endogenous grid points $\mathcal{M}_t$ will not be monotone in end-of-period housing - see Figure (5).This is because as agents become wealthier, they will reach a threshold where they anticipate upgrading their housing stock sometimes in the future. At this threshold, they also expect to discontinuously decrease future non-housing consumption, causing a jump up in the RHS of (45). As a result, they will discontinuously decrease current period housing consumption.

Moreover, the optimal housing policy that takes into account the future sequence of adjustment decisions will be non-monotone. Nonetheless, as discussed in Section 5.1, we can set $\bar{J} = 1$ and $\rho_r > \frac{2\epsilon}{\text{MPC}}$. We can also set end-of-period housing assets $a \mapsto \hat{\text{y}}_{h,t}(a)$ and consumption $a \mapsto \hat{\text{c}}_t(a)$ as the grid pasting function κ_t for adjusters and non-adjusters, respectively.

5.2.4. *Numerical implementation.* To parameterize the model, we set $\rho = 3$, $\alpha = 0.66$, $\beta = .93$, $\tau = .18$, $r = 0.01$, and $T = 60$. We assume $\tilde{w}_t$ is the earnings function for females in Dobrescu et al. (2018), with $w_t = \tilde{w}_t(\tilde{z})$ and $\tilde{\eta}$ being a random variable taking values in $\{0.1, 1\}$ with equal probability; for simplicity, earnings shocks are i.i.d . To benchmark our method with the others, we will implement the solution algorithm using VFI, EGM with RFC, and the nested EGM method in Druedahl (2021). As the financial assets and total resources grids are one-dimensional, we use standard linear interpolation to implement all methods. To implement RFC, when the endogenous grid is one-dimensional, we find it is more efficient to proceed sequentially instead of computing the tangent plane between each point and its neighbours. In particular, we proceed from the lowest endogenous grid point $m^{\#}_{0,t}$ and apply RFC to the neighbouring point $m^{\#}_{1,t}$. If $m^{\#}_{1,t}$ is sub-optimal, we delete the point and test $m^{\#}_{2,t}$ from $m^{\#}_{0,t}$. If $m^{\#}_{1,t}$ point is optimal, we move to $m^{\#}_{1,t}$ and apply RFC to test $m^{\#}_{2,t}$. The procedure is repeated sequentially until all sub-optimal points are removed.[36]

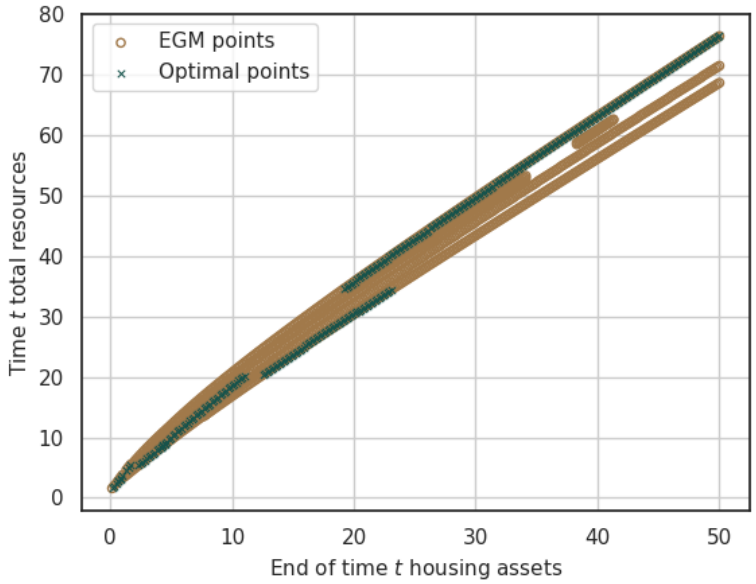

Figure 5. Endogenous total resources plotted on an exogenous grid

Figure 5 shows the map of endogenous grid points to the exogenous grid for a 59 year old, with the exogenous grid points belonging to a subset of a collection of one-dimensional spaces, each corresponding to a particular future sequence of discrete choices. Despite the irregular grid and non-monotonicity of the optimal policy, Figure 6 shows how the RFC algorithm recovers the optimal points by zooming in on the top right section of the exogenous grid.

[36]Our online repository contains implementations of both the sequential and non-sequential versions for completeness.

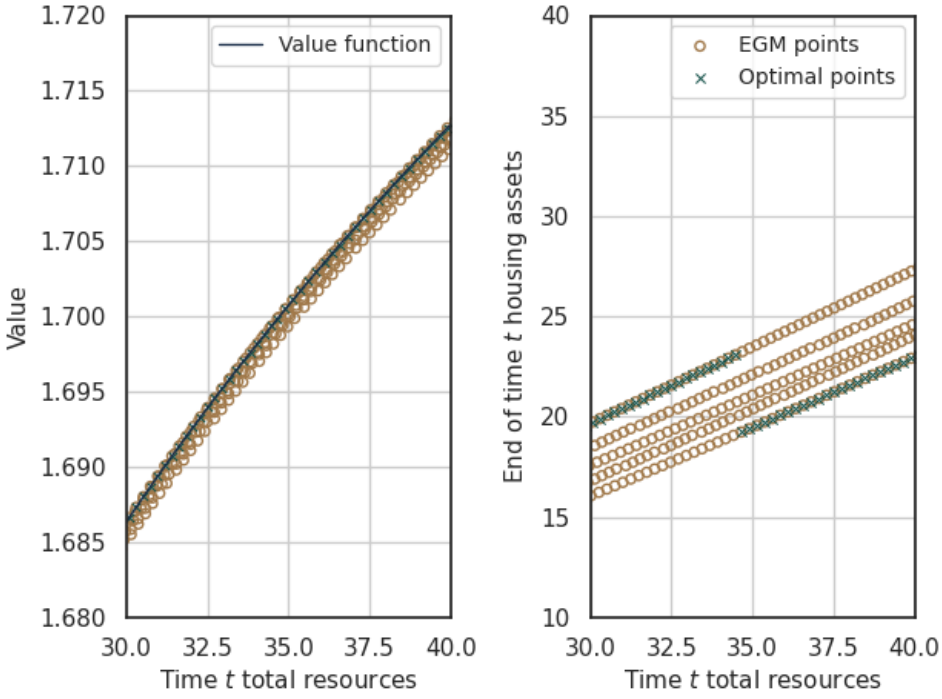

Figure 6. Value function and optimal housing policy function for the top right section of the endogenous grid

Finally, the left plot of Figure 7 compares computational speed across methods, and shows that despite the intermediate root-finding step, EGM with RFC (i) still outperforms VFI by a factor of more than 20, and (ii) is comparable in scale with NEGM but still 25% faster. As expected, since EGM with root finding uses all the information contained in the Euler equation to compute the optimal policy, the right plot of Figure 7 shows that our RFC algorithm delivers up to an order of magnitude improvement in accuracy over both VFI and NEGM.

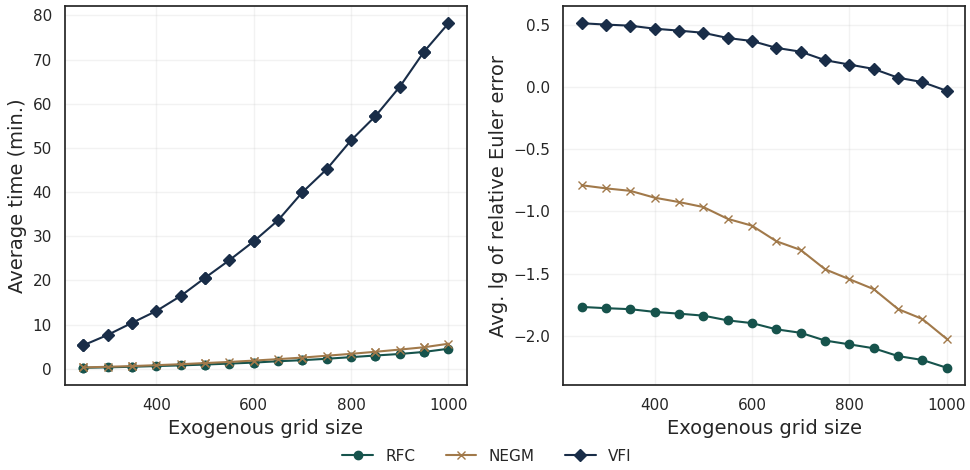

Figure 7. Computational speed and Euler error benchmarking

6. Conclusions

This study resolves several critical challenges in applying dynamic programming methods to solve multidimensional stochastic optimization models with discrete-continuous choices and occasionally binding constraints. Our contribution enables a rigorous and systematic implementation of the inverse Euler equation to maximize the use of first order information to solve such models efficiently. In particular, by introducing the S-function, we establish a general and straightforward way to derive the necessary Euler equation in all classes of models with non-compact feasibility correspondences, unbounded rewards, occasionally binding constraints, and discrete choices. We are also the first to provide verifiable conditions on the model primitives that determine when the inverse Euler equation is well-defined. Additionally, our RFC algorithm offers a highly efficient and accurate avenue to solve discrete-continuous problems. This algorithm is not only compatible with vectorized, high-performance computing but also introduces verifiable error bounds for the inverse Euler equation methods applied to models with and without discrete choices. We finally demonstrate the practical impact of our contributions via two workhorse applications, with a special focus on the RFC gains in computational speed and accuracy, as well as the ability of our approach to handle multidimensional problems that could not be previously solved using EGM.

One topic we plan to tackle next concerns introducing model uncertainty in our definition of the inverse optimization problems. Our setup so far assumed the exogenous grid was observed 'as if' it was the result of a model-consistent behavior given the deeper structural parameters. However, the current literature on inverse optimization incorporates various methods to minimize the uncertainty related to observed variables being model-consistent (Bertsimas et al., 2015; Ghobadi et al., 2018; Chan et al., 2023). Understanding the implications of these advancements in inverse optimization for dynamic structural estimation is a key area of further work.

References

Achdou, Y., Han, J., Lasry, J.-M., Lions, P.-L., and Moll, B. (2021). Income and wealth distribution in macroeconomics: A continuous-time approach. *The Review of Economic Studies*, 89(1):45–86.

Aiyagari, S. R. (1994). Uninsured idiosyncratic risk and aggregate saving. *The Quarterly Journal of Economics*, 109(3):659–684.

Alfaro, I., Bloom, N., and Lin, X. (2024). The finance uncertainty multiplier. *Journal of Political Economy*, 132(2):577–615.

Arellano, C. (2008). Default risk and income fluctuations in emerging economies. *American Economic Review*, 98(3):690–712.

Arellano, C., Maliar, L., Maliar, S., and Tsyrennikov, V. (2016). Envelope condition method with an application to default risk models. *Journal of Economic Dynamics and Control*, 69:436–459.

Attanasio, O., Levell, P., Low, H., and Sanchez-Marcos, V. (2018). Aggregating elasticities: Intensive and extensive margins of women's labor supply. *Econometrica*, 86(6):2049–2082.

Auclert, A., Bardóczy, B., Rognlie, M., and Straub, L. (2021). Using the sequence-space Jacobian to solve and estimate heterogeneous-agent models. *Econometrica*, 89(5):2511–2547. Citations: 25.

Bardoćzy, B. (2022). Spousal insurance and the amplification of business cycles. *Working Paper*.

Barillas, F. and Fernandez-Villaverde, J. (2007). A generalization of the endogenous grid method. *Journal of Economic Dynamics and Control*, 31(8):2698–2712.

Beraja, M. and Zorzi, N. (2023). On the size of stimulus checks: How much is too much? *Working Paper*.

Berger, D. and Vavra, J. (2015). Consumption dynamics during recessions. *Econometrica*, 83(1):101–154.

Bertsimas, D., Gupta, V., and Paschalidis, I. C. (2015). Data-driven estimation in equilibrium using inverse optimization. *Mathematical Programming*, 153(2):595–633.

Best, M. C., Cloyne, J. S., Ilzetzki, E., and Kleven, H. J. (2019). Estimating the elasticity of intertemporal substitution using mortgage notches. *The Review of Economic Studies*, 87(2):656–690.

Bewley, T. F. (1972). Existence of equilibria in economies with infinitely many commodities. *Journal of Economic Theory*, 4(3).

Borovkov, A. A. (2013). *Stochastic recursive sequences*, pages 507–526. Springer London, London.

Brumm, J. and Scheidegger, S. (2017). Using adaptive sparse grids to solve high-dimensional dynamic models. *Econometrica*, 85(5):1575–1612.

Buera, F. J. and Moll, B. (2015). Aggregate implications of a credit crunch: The importance of heterogeneity. *American Economic Journal. Macroeconomics*, 7(3):1–42.

Cao, D. (2020). Recursive equilibrium in Krusell and Smith (1998). *Journal of Economic Theory*, 186:104978.

Carroll, C. D. (1997). Buffer-stock saving and the life cycle/permanent income hypothesis. *The Quarterly Journal of Economics*, 112(1):1–55.

Carroll, C. D. (2006). The method of endogenous gridpoints for solving dynamic stochastic optimization problems. *Economics Letters*, 91(3):312–320.

Carroll, C. D. (2023). Theoretical foundations of buffer stock saving. *Working paper*.

Chan, T. C. Y., Mahmood, R., and Zhu, I. Y. (2023). Inverse optimization: Theory and applications. *Operations Research*, Preprint(Preprint):Preprint.

Chen, L. and Xu, J.-c. (2004). Optimal Delauny triangulations. *Journal of Computational Mathematics*, 22(2):299–308.

Clausen, A. and Strub, C. (2020). Reverse calculus and nested optimization. *Journal of Economic Theory*, 187.

Cocco, J. F. (2005). Portfolio choice in the presence of housing. *The Review of Financial Studies*, 18(2):535–567.

Coleman, W. J. (1990). Solving the stochastic growth model by policy-function iteration. *Journal of Business and Economic Statistics*, 8(1):27–29.

Cooper, I. (2006). Asset pricing implications of nonconvex adjustment costs and irreversibility of investment. *Journal of Finance*, 61(1):139–170.

Cosar, A. K. and Green, E. J. (2014). Necessary and sufficient conditions for dynamic optimization. *Macroeconomic Dynamics*, FirstView:1–18.

Crawford, R. and O'Dea, C. (2020). Household portfolios and financial preparedness for retirement. *Quantitative Economics*, 11(2):637–670.

Dávila, J., Hong, J. H., Krusell, P., and Ríos-Rull, J.-V. (2012). Constrained efficiency in the neoclassical growth model with uninsurable idiosyncratic shocks. *Econometrica*, 80(6):2431–2467.

Deaton, A. (1991). Saving and liquidity constraints. *Econometrica*, 59(5):1221.

Dechert, W. (1982). Lagrange multipliers in infinite horizon discrete time optimal control models. *Journal of Mathematical Economics*, 9:285–302.

Dobrescu, L., Motta, A., and Shanker, A. (2024). The power of knowing a woman is in charge: Lessons from a randomized experiment. *Management Science*, Pre-print(0):null.

Dobrescu, L. and Shanker, A. (2023). Fast upper-envelope scan for discrete-continuous dynamic programming. *SSRN Electronic Journal 4181302*.

Dobrescu, L. I., Fan, X., Bateman, H., Newell, B. R., and Ortmann, A. (2018). Retirement savings: A tale of decisions and defaults. *Economic Journal*, 128:1047–1094.

Dobrescu, L. I., Shanker, A., Bateman, H., Newell, B. R., and Thorp, S. (2022). Eggs and baskets: Lifecycle portfolio dynamics. *SSRN Working Paper No. 4069226*.

Druedahl, J. (2021). A guide on solving non-convex consumption-saving models. *Computational Economics*, 58:747–775.

Druedahl, J. and Jørgensen, T. H. (2017). A general endogenous grid method for multi-dimensional models with non-convexities and constraints. *Journal of Economic Dynamics and Control*, 74:87–107.

Duarte, V., Duarte, D., Fonseca, J., and Montecinos, A. (2020). Benchmarking machine-learning software and hardware for quantitative economics. *Journal of Economic Dynamics and Control*, 111:103796.

Fagereng, A., Gottlieb, C., and Guiso, L. (2017). Asset market participation and portfolio choice over the life-cycle. *Journal of Finance*, 72(2):705–750.

Fagereng, A., Holm, M. B., Moll, B., and Natvik, G. (2019). Saving behavior across the wealth distribution: The importance of capital gains. Working Paper 26588, National Bureau of Economic Research.

Feinberg, E. A., Kasyanov, P. O., and Zadoianchuk, N. V. (2012). Average cost Markov decision processes with weakly continuous transition probabilities. *Mathematics of Operations Research*, 37(4):591–607.

Fella, G. (2014). A generalized endogenous grid method for non-smooth and non-concave problems. *Review of Economic Dynamics*, 17:329–344.

Fernández-Villaverde, J., Hurtado, S., and Nuño, G. (2023). Financial frictions and the wealth distribution. *Econometrica*, 91(3):869–901.

French, E. (2005). The effects of health, wealth, and wages on labour supply and retirement behaviour. *Review of Economic Studies*, 72(2):395–427.

Ghobadi, K., Lee, T., Mahmoudzadeh, H., and Terekhov, D. (2018). Robust inverse optimization. *Operations Research Letters*, 46(3):339–344.

González-Sánchez, D. and Hernández-Lerma, O. (2013). On the Euler equation approach to discrete–time nonstationary optimal control problems. *Journal of Dynamics and Games*, 1(1):57–78.

Gourinchas, P. O. and Parker, J. A. (2002). Consumption over the life cycle. *Econometrica*, 70(1):47–89.

Hai, R. and Heckman, J. J. (2019). A dynamic model of health, addiction, education, and wealth. Working Paper 2688384, Becker Friedman Institute for Research in Economics. University of Miami Business School Research Paper No. 2688384.

Harris, C. R., Millman, K. J., van der Walt, S. J., Gommers, R., Virtanen, P., Cournapeau, D., Wieser, E., Taylor, J., Berg, S., Smith, N. J., Kern, R., Picus, M., Hoyer, S., van Kerkwijk, M. H., Brett, M., Haldane, A., del Río, J. F., Wiebe, M., Peterson, P., Gérard-Marchant, P., Sheppard, K., Reddy, T., Weckesser, W., Abbasi, H., Gohlke, C., and Oliphant, T. E. (2020). Array programming with NumPy. *Nature*, 585(7825):357–362.

Hernandez-Lerma, O. and Lasserre, J. (2012). *Discrete-time Markov control processes: Basic optimality criteria*. Stochastic modelling and applied probability. Springer New York.

Huggett, M. (1996). Wealth distribution in life-cycle economies. *Journal of Monetary Economics*, 38(3):469–494.

Hull, I. (2015). Approximate dynamic programming with post-decision states as a solution method for dynamic economic models. *Journal of Economic Dynamics and Control*, 55:57–70.

Iskhakov, F. (2015). Multidimensional endogenous gridpoint method: Solving triangular dynamic stochastic optimization problems without root-finding operations. *Economics Letters*, 135:72–76.

Iskhakov, F., Jørgensen, T. H., Rust, J., and Schjerning, B. (2017). The endogenous grid method for discrete-continuous dynamic choice models with (or without) taste shocks. *Quantitative Economics*, 8(2):317–365.

Iskhakov, F. and Keane, M. (2021). Effects of taxes and safety net pensions on life-cycle labor supply, savings and human capital: The case of australia. *Journal of Econometrics*, 223(2):401–432. Annals issue: Implementation of Structural Dynamic Models.

Iyengar, G. and Kang, W. (2005). Inverse conic programming with applications. *Operations Research Letters*, 33(3):319–330.

Jang, Y. and Lee, S. (2023). A generalized endogenous grid method for default risk models. *SSRN Electronic Journal 3442070*.

Kaplan, G., Mitman, K., and Violante, G. L. (2020). The housing boom and bust: Model meets evidence. *Journal of Political Economy*, 128(9):3285–3345.

Kaplan, G., Moll, B., and Violante, G. L. (2018). Monetary policy according to hank. *American Economic Review*, 108(3):697–743.

Kaplan, G. and Violante, G. L. (2014). A model of the consumption response to fiscal stimulus payments. *Econometrica*, 82(4):1199–1239.

Kekre, R. (2022). Unemployment insurance in macroeconomic stabilization. *The Review of Economic Studies*, 90(5):2439–2480.

Khan, A. and Thomas, J. K. (2008). Idiosyncratic shocks and the role of nonconvexities in plant and aggregate investment dynamics. *Econometrica*, 76(2):395–436.

Krueger, D., Mitman, K., and Perri, F. (2016). Chapter 11 - Macroeconomics and household heterogeneity. In Taylor, J. B. and Uhlig, H., editors, *Handbook of Macroeconomics*, volume 2, pages 843–921. Elsevier.

Krusell, P. and Smith, A. A. (1998). Income and wealth heterogeneity in the macroeconomy. *Journal of Political Economy*, 106(5):867–896.

Laibson, D., Maxted, P., and Moll, B. (2021). Present bias amplifies the household balance-sheet channels of macroeconomic policy. *NBER Working Paper No. 29094*.

Li, H. and Stachurski, J. (2014). Solving the income fluctuation problem with unbounded rewards. *Journal of Economic Dynamics and Control*, 45:353–365.

Ludwig, A. and Schön, M. (2018). Endogenous grids in higher dimensions: Delaunay interpolation and hybrid methods. *Computational Economics*, 51(3):463–492.

Lujan, A. (2023). EGM^n: The sequential endogenous grid method. *Working paper*.

Ma, Q., Stachurski, J., and Toda, A. A. (2022). Unbounded dynamic programming via the Q-transform. *Journal of Mathematical Economics*, 100:102652.

Maliar, L. and Maliar, S. (2013). Envelope condition method versus endogenous grid method for solving dynamic programming problems. *Economics Letters*, 120(2):262–266.

Maliar, L., Maliar, S., and Winant, P. (2021). Deep learning for solving dynamic economic models. *Journal of Monetary Economics*, 122:76–101.

Marimon, R. and Werner, J. (2021). The envelope theorem, Euler and Bellman equations, without differentiability. *Journal of Economic Theory*, 196:105309.

Pröhl, E. (2023). Existence and uniqueness of recursive equilibria with aggregate and idiosyncratic risk. *SSRN Electronic Journal 3250651*.

Reffett, K. L. (1996). Production-based asset pricing in monetary economies with transactions costs. *Economica*, 63(251):427–443.

Rendahl, P. (2015). Inequality constraints and euler equation-based solution methods. *Economic Journal*, 125(585):1110–1135.

Rincón-Zapatero, J. P. and Santos, M. S. (2009). Differentiability of the value function without interiority assumptions. *Journal of Economic Theory*, 144(5):1948–1964.

Rust, J. (1987). Optimal replacement of GMC bus engines: An empirical model of Harold Zurcher. *Econometrica*, 55(5):999–1033.

Sargent, T. J. and Stachurski, J. (2023). Completely abstract dynamic programming. *Working Paper*, 2308.02148:1–37.

Sargent, T. J. and Stachurski, J. (2024). Quantitative economics with python using jax: An introduction to jax. `https://jax.quantecon.org/jax_intro.html`. Accessed: 2024-05-07.

Shanker, A. (2017). Existence of recursive constrained optima in the heterogenous agent neoclassical growth model. *Working Paper*.

Sorger, G. (2015). *Dynamic economic analysis: Deterministic models in discrete time*. Cambridge University Press.

Stachurski, J. (2022). *Economic dynamics: Theory and computation, second edition*. MIT Press.

White, M. (2015). The method of endogenous gridpoints in theory and practice. *Journal of Economic Dynamics and Control*, 60:26–41.

Yogo, M. (2016). Portfolio choice in retirement: Health risk and the demand for annuities, housing, and risky assets. *Journal of Monetary Economics*, 80:17–34.